Regions of Interest on Ganymede's and Callisto's surfaces as potential targets for ESA's JUICE mission

K. Stephan[1], T. Roatsch[1], F. Tosi[2], K.-D. Matz[1], E. Kersten[1], R. Wagner[1], P. Molyneux[3], P. Palumbo[2,4], F. Poulet[5], H. Hussmann[1], S. Barabash[6], L. Bruzzone[7], M. Dougherty[8], R. Gladstone[3], L.I. Gurvits[9,10], P. Hartogh[11], L. Iess[12], J.-E. Wahlund[13], P. Wurz[14], O. Witasse[15], O. Grasset[16], N. Altobelli[15], J. Carter[4], T. Cavalié[17,18], E. d'Aversa[2], V. Della Corte[2], G. Filacchione[2], A. Galli[14], V. Galluzzi[2], K. Gwinner[1], E. Hauber[1], R. Jaumann[19], K. Krohn[1], Y. Langevin[4], A. Lucchetti[20], A. Migliorini[2], G. Piccioni[2], A. Solomonidou[21], A. Stark[1], G. Tobie[16], C. Tubiana[2], C. Vallat[22], T. Van Hoolst[23,24], and the JUICE SWT team.

[1] Institute of Planetary Research, German Aerospace Center (DLR), 14489 Berlin, Germany,
[2] Istituto Nazionale di AstroFisica – Istituto di Astrofisica e Planetologia Spaziali (INAF-IAPS), Via del Fosso del Cavaliere 100, 00133 Rome, Italy,
[3] Southwest Research Institute, 6220 Culebra Road, San Antonio, Texas, 78238, USA,
[4] Università degli Studi di Napoli "Parthenope", Napoli, Italy,
[5] Institut d'Astrophysique Spatiale, Univ. Paris Sud / CNRS (Bat. 121, Orsay Campus, 91405 Orsay, France,
[6] The Swedish Institute of Space Physics, Box 812, SE-981 28 Kiruna, Sweden,
[7] Università degli Studi di Trento, Via Sommarive, 9 I-38123, Trento, Italy,
[8] Imperial College London, United Kingdom,

[9] Joint Institute for VLBI ERIC, Oude Hoogeveensedijk 4, 7991 PD Dwingeloo, The Netherlands,
[10] Department of Astrodynamics and Space Missions, Delft University of Technology, Kluyverweg 1, 2629 HS Delft, The Netherlands,
[11] Max-Planck-Institut für Sonnensystemforschung, Germany,
[12] University La Sapienza of Rome, via Eudossiana 18, 00186 Roma, Italy,
[13] Swedish Institute of Space Physics, Box 537, 751 21 Uppsala, Sweden
[14] Universität Bern, Physikalisches Institut, Weltraum und Planetologie, Sidlerstr. 5, 3012 Bern, Switzerland,
[15] European Space Research and Technology Centre (ESTEC), European Space Agency (ESA), 2200 AG Noordwijk, Netherlands,
[16] Laboratoire de Planétologie et Géodynamique, UMR-CNRS 6112, Université de Nantes, BP 92208, 44322 Nantes Cedex 3, France,
[17] Laboratoire d'Astrophysique de Bordeaux, Univ. Bordeaux, CNRS, B18N, Allée Geo roy Saint-Hilaire, 33615 Pessac, France,
[18] LESIA, Observatoire de Paris, PSL Research University, CNRS, Sorbonne Universités, UPMC Univ. Paris 06, Univ. Paris Diderot, Sorbonne Paris Cité, Meudon, France,
[19] Free University Berlin, Planetary Science and Remote Sensing, Malteserstr. 74-100, 12249 Berlin,
[20] INAF-Osservatorio Astronomico di Padova, Vicolo dell' Osservatorio 5, 35122 Padova, Italy,
[21] California Institute of Technology, Pasadena, CA, 91125, USA,
[22] RHEA group for ESA/ESAC, 28, Villanueva de la Cañada, 28692, Madrid, Spain

[23] Royal Observatory of Belgium, Brussels, Belgium,

[24] Instituut voor Sterrenkunde, KU Leuven, Belgium.

Corresponding author: Katrin Stephan (Katrin.Stephan@dlr.de).

Abstract

The JUpiter Icy moons Explorer (JUICE) will investigate Ganymede's and Callisto's surfaces and subsurfaces from orbit to explore the geologic processes that have shaped and altered their surfaces by impact, tectonics, possible cryovolcanism, space weathering due to micrometeorites, radiation and charged particles as well as explore the structure and properties of the icy crust and liquid shell (Grasset et al., 2013). The best possible synergy of the JUICE instruments is required to answer the major science objective of this mission and to fully exploit the potential of the JUICE mission. Therefore, the JUICE team is aiming to define high priority targets on both Ganymede's and Callisto's surfaces to support the coordination of the planning activities by the individual instrument teams. Based on the science objectives of the JUICE mission and the most recent knowledge of Ganymede's and Callisto's geologic evolution we propose a collection of Regions of Interest (RoIs), which characterize surface features and terrain types representing important traces of geologic processes, from past and/or present cryovolcanic and tectonic activity to space weathering processes, which are crucial to understand the geologic evolution of Ganymede and Callisto. The proposed evaluation of RoIs is based on their scientific importance as well as on the opportunities and conditions to observe them during the currently discussed mission profile.

Keywords

JUICE mission, Ganymede, Callisto, surface features, target regions, observation planning

1 Introduction

The JUpiter ICy moons Explorer (JUICE) is the first large-class mission selected in the framework of the European Space Agency's (ESA) Cosmic Vision 2015-2025 programme with the purpose of expanding our understanding on: 1) what are the conditions for planet formation and the emergence of life, and 2) how does the Solar System works (ESA JUICE definition study report /Red Book, 2014; Grasset et al., 2013). With its powerful remote sensing, geophysical, and in situ payload complement, JUICE will provide the most comprehensive exploration of the Jovian system (ESA JUICE definition study report /Red Book, 2014; Grasset et al., 2013). A central part of the mission is the investigation of Jupiter's satellite Ganymede as a planetary body and potential habitat, with JUICE being the first spacecraft orbiting around an extra-terrestrial satellite. Ganymede is not only the largest satellite in the Solar System, but it is also the only satellite that shares major characteristics of terrestrial planets in terms of size, metallic and liquid core, and its unique magnetic and plasma interaction with the surrounding Jovian environment. Thus, the expected results regarding Ganymede's origin and evolution will not only be a key to unveiling the diversity among the bodies in the Jovian system and the Solar System, but will also contribute to our understanding of the broad diversity of exoplanets, which possibly also include icy planets and moons. Additionally, the JUICE spacecraft will perform several flybys at Callisto and two at Europa, which, like Ganymede, are believed to hide a global ocean below their icy crust. These

flybys will deepen our understanding on the current state and evolution of the Jovian satellite system and will complete a comparative picture of the Galilean satellites and their potential habitability.

The JUICE spacecraft will carry a powerful payload consisting of 10 state-of-the-art instruments plus one experiment that combines the spacecraft's radio communication system with ground-based instruments. The remote sensing package includes multispectral- and hyperspectral-imaging capabilities from the ultraviolet to the sub-millimetre wavelengths: the optical camera system JANUS (Jovis, Amorum ac Natorum Undique Scrutator) (Della Corte et al., 2019; Della Corte et al., 2014; Palumbo et al., 2014), the visible and near infrared imaging spectrometer MAJIS (Moons and Jupiter Imaging Spectrometer) (Langevin and Piccioni, 2017; Langevin et al., 2018; Piccioni et al., 2019), the UV imaging spectrograph (UVS) (Gladstone et al., 2013), and the Sub-millimeter Wave Instrument (SWI) (Hartogh et al., 2013). The geophysical package consists of the laser altimeter GALA (GAnymede Laser Altimeter) (Hussmann et al., 2019; Hussmann et al., 2013), and the radar sounder RIME (Radar for Icy Moons Exploration) (Bruzzone and Croci, 2019; Bruzzone et al., 2013) for exploring the surfaces and subsurfaces of the moons, and the radio science experiment 3GM (Gravity & Geophysics of Jupiter and Galilean Moons) (Cappuccio et al., 2020; Iess, 2013) to perform measurements of the gravity field and to probe the atmospheres of Jupiter and its satellites. The in situ suite comprises a powerful package to study the particle environment (PEP) (Barabash et al., 2016) consisting of 6 instruments that can measure ions, electrons, and thermal neutrals (Wurz et al., 2018), the JUICE magnetometer (J-MAG) (Dougherty and al., 2014) and the radio and plasma wave instrument (RPWI) (Bergman et al., 2017), including electric fields sensors and a Langmuir probe. The Planetary Radio Interferometry and Doppler Experiment (PRIDE) (Dirkx et al., 2017; Gurvits et al., 2013) will be using ground-based radio

telescopes in Very Long Baseline Interferometry (VLBI) (Dirkx et al., 2017) and single-antenna Doppler regimes to help together with 3GM (Di Benedetto et al., 2021; Fabrizio et al., 2021; Iess, 2013) to precisely determine the spacecraft state vector, but will also be involved in a support role for a variety of applications such as to monitor Ganymede's and Europa's tidal characteristics.

This payload is capable of addressing all of the mission's science goals, from in situ measurements of Jupiter's atmosphere and plasma environment, to remote observations of the surface and interior of all three icy moons (Grasset et al., 2013). Nevertheless, the best possible synergy of the JUICE instruments during the mission in the Jupiter system is needed, which requires a careful consideration of the observations strategies by each instrument team. Furthermore, the expected illumination conditions at the specific target, the specific instrument's observation capabilities and the coverage and/or data volume limitations during the closest flybys and orbit phases might constrain the ability to completely observe the surfaces of Ganymede as well as Callisto with the highest quality by the instruments onboard the JUICE spacecraft. For this reason, a definition of scientific regions of interest (RoIs) is required to exploit the full potential of the JUICE mission. Therefore, to support the observation planning activities of the JUICE team and the individual instrument teams during flybys and orbit phases, we propose a selection of high priority RoIs on Ganymede's and Callisto's surface, which represent key regions and features to investigate the evolution of these bodies and the interaction with possible ocean material and the magnetosphere of Jupiter.

Following a description of the JUICE mission (section 2), we introduce the RoI selection and organization procedure (section 3) followed by a description of the selected RoIs (section 4) including their importance for the JUICE mission, the state-of-the-art knowledge, the so far unanswered scientific questions and the required observation parameters to answer the open

scientific questions and to fulfil the science objectives of the JUICE mission. We conclude with an outlook for the use of the selected RoIs and their application for the JUICE planning activities (section 5).

2 JUICE mission

Currently planned for a launch no earlier than September 2022, JUICE would arrive in the Jovian system in July 2031 and spend more than three years making detailed observations of the giant gaseous planet Jupiter and its three icy Galilean moons: Ganymede, Callisto and Europa, before entering orbit around Ganymede.

Table 1 summarizes the mission scenario based on the latest Consolidated Report on Mission Analysis (CReMA, version 4.2b22.1, option 150l0a, (Boutonnet et al., 2018)). It should be noted that the JUICE mission scenario was updated only recently. The JUICE Science Working Team (SWT) and the JUICE scientific Working Groups (WGs) have been using an older mission profile, namely CReMA 3.0 released in 2015 (Tab. 2), as a baseline trajectory to perform a top-level analysis and to estimate the scientific return expected for the various mission phases and this has also been used as background information for the selection of the proposed lists of potential target areas.

Cruise/Tour/Orbit	Phase	Distance at closest approach	Start	End
Cruise			09/2022	07/2031
Jupiter Tour				
	Jupiter Orbit Insertion (JOI) Jupiter Equatorial Phase 1 "Approach and first ellipse" / Phase 2 "Energy reduction" (2 Ganymede flybys, 1 Callisto flyby)	Ganymede 401 km / Callisto 3544 km	07/2031	06/2032
	Phase 3 "Europa flybys" (2 Europa flybys)	Europa 400 km	06/2032	07/2032
	Phase 4 "Jupiter high latitude" (16 Callisto flybys)	Callisto 200 km	07/2032	08/2033
	Phase 5 "Low energy / Transfer to Ganymede" (8 Ganymede flybys, 3 Callisto flybys)	Ganymede 866 km / Callisto 401 km	08/2033	12/2034
Ganymede Orbit	Phase 6			
	GEOa: Elliptical Orbit #1	200 km	12/2034	01/2035
	GCO5000 - High Altitude (circular)	~5100 km	01/2035	04/2035
	GEOb: Elliptical Orbit #2	~600 km	04/2035	05/2035
	GCO500 - Intermediate Altitude (circular)	~490 km	05/2035	10/2035
	GCO200 - Potential Extended Mission: Low Altitude (circular)	~200 km	10/2035	11/2035

Table 1: JUICE mission scenario based on CReMA 4.2b22.1, option 150l0a. Please note that only the distant of the closest approach among all flybys of a given mission phase are indicated.

Cruise/Tour	Phase	Distance at closest approach	Start	End
Cruise			06/2022	04/2029
Jupiter Tour				
	Jupiter Orbit Insertion (JOI) Jupiter Equatorial Phase 1 / Transfer to Callisto / **3 close Ganymede flybys**	Callisto 199 km Ganymede 401 / 401 / 502 km	04/2029	10/2030
	Europa Phase: 2 Europa flybys, **3 Callisto flybys**	Europa 403 km Callisto 199 km	10/2030	11/2030
	Jupiter High Latitude Phase with **9 Callisto flybys**	Callisto 199 km	11/2030	07/2031
	Jupiter Equatorial Phase 2 / Transfer to Ganymede		07/2031	08/2032
Ganymede Tour				
	Elliptical Orbit #1	213 km	08/2032	09/2032
	GCO 5000 - High Altitude (circular)	~5000 km	09/2032	11/2032
	Elliptical Orbit #2		11/2032	12/2032
	GCO 500 - Intermediate Altitude (circular)	~500 km	12/2032	06/2033
	GCO 200 - Potential Extended Mission: Low Altitude (circular)	~200 km	06/2033	07/2033

Table 2: JUICE mission scenario based on CReMA 3.0. Please note that only the distant of the closest approach among all flybys of a given mission phase are indicated.

The transition from one mission profile to another is not without consequences: apart from the launch date and the duration of the cruise phase, the Jupiter tour may also substantially change, e.g. in terms of the total number of Callisto flybys, the inclination of the JUICE orbital plane during the moderate inclination phase around Jupiter, and the solar illumination conditions during flybys, perijoves, and at the time of the Ganymede orbit insertion. On the other hand, other mission phases

are substantially unchanged: for example, the second phase of the Jupiter tour called "Energy reduction" always includes at least two flybys of Ganymede (3 Ganymede flybys for CReMA 3.0 and four for CReMA 4.2b22.1) and one flyby of Callisto, while the third phase of the tour called "Europa flybys" always foresees two close flybys of Europa at a minimum altitude of 400 km over the surface two weeks from each other. Regardless of the mission profile, close flybys of Ganymede and Callisto can have minimum altitudes over the surface of 400 km and 200 km, respectively. Although, the flybys are untouched in terms of lowest altitude, the regions overflown are affected by the change of trajectory and the illumination conditions are a bit less favorable with the new trajectory (see section 2.1).

In the sixth and salient phase of the mission, JUICE will finally enter orbit around Ganymede and stay there for at least nine months, first following an elliptical orbit, that naturally evolves in a high circular orbit at about 5100 km from the surface (GCO5000) and a second elliptical phase and finally descending, with an orbital manoeuvre, to a circular orbit at about 500 km altitude (GCO500). At the end of this 500-km phase, if the energy budget allows it, in principle JUICE might descend on a further lower circular orbit with an altitude of about 200 km in height, for one month before crashing onto the surface of Ganymede (Tab. 2). While for Europa observation the strategy is simply to observe as much as possible during the two only flybys, the multiple flybys at Ganymede and Callisto and the final orbital phases at Ganymede will allow performing a much more complex and target-oriented observation plan. The work on a list of potential RoIs for each of these satellites originated from the possibility to perform high resolution observations of specific pre-selected targets, which would fully exploit the potential of the JUICE mission.

2.1 Ganymede flybys, GEO and GCO5000

Global mapping of Ganymede by the JUICE remote sensing instruments from the UV to the sub-millimeter wavelengths is envisaged during the previous flybys, the elliptical phase and the high altitude GCO5000 prior to GCO500 providing full coverage of Ganymede's surface at moderate spatial resolutions.

a) JANUS

During the flyby configurations that are currently in discussion for JUICE, mainly the anti-Jovian hemisphere of Ganymede's surface can be observed by the imaging and spectral imaging JUICE instruments. Particularly, JANUS images will achieve spatial resolutions of ~200 m/pixel comparable to medium-resolved Galileo SSI images and could enable a first look into the equatorial region of the RoIs in the ancient terrain of *Marius Regio* and the neighbouring portions of the bright terrain (Fig. 1). During GCO5000 JANUS images will reach spatial resolutions up to ~ 77 m per pixel (possibly followed by a 4 x 4 binning or compression). At closest approach of JUICE during the Ganymede flybys, JANUS can observe the surface only in panchromatic mode. Otherwise, Ganymede's surface will be observed with four colour filters or eight colour filters, whose central 15 wavelengths range between 380 and 1015 nm (Palumbo et al., 2014). Stereo imaging at Ganymede could be enabled by combining nadir and S/C tilted observations. However, the current trajectory will not allow to achieve both, a global coverage in panchromatic mode and considerable number of stereo images.

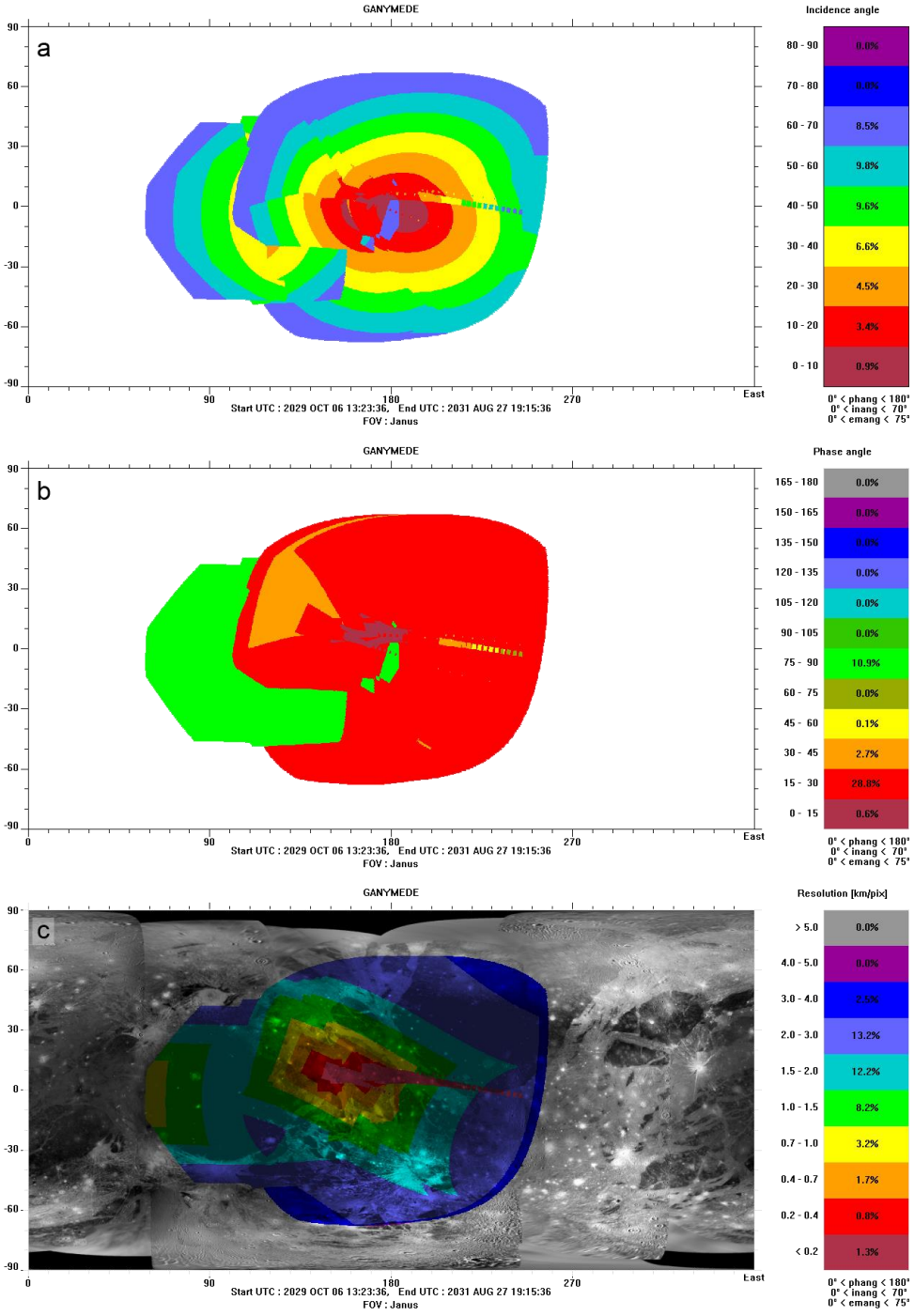

Figure 1: JANUS coverage (nadir looking only) during the Ganymede flybys based on CReMA 3.0: a) incidence angle, b) phase angle and c) spatial resolution overlaid on the global USGS base map.

b) MAJIS

MAJIS will provide spectral imaging of Ganymede in the overall range from the visible to the near-infrared using two separate channels (VIS-NIR channel: 0.5-2.35 μm, average spectral sampling 3.7 nm; IR channel: 2.25-5.54 μm, average spectral sampling: 6.5 nm) and will characterize the composition and physical properties of Ganymede's surface and relationships between the surface and the external environment (Langevin and Piccioni, 2017; Piccioni et al., 2019). Regions of interest will targeted during close flybys; binning and onboard compression will be routinely used to reduce the data volume as needed. MAJIS is a slit spectrometer with a FOV defined by a single slit (0.0086° x 3.4°). To build a hyperspectral image, *N* slits have to be acquired one after the other using either a scanning mirror or the motion of the spacecraft, which may take tens of minutes depending on the size of the image to build. During GCO5000, MAJIS should be able to achieve nearly global or broadly regional coverage of Ganymede with an average spatial resolution of ~ 3 km per pixel using spatial binning x4, provided that the solar illumination conditions are favourable enough.

It has to be noted that based on CReMA 3.0 the majority of equatorial areas would be observed with incidence and phase angles <45°, which is optimal for colour and compositional studies of Ganymede's surface by JANUS and the other spectral imaging instruments such as MAJIS. However, the natural precession of the orbital plane with respect to the direction of Sun would result to progressively less favourable illumination conditions for the orbital mission with incidence angles of about 80° and larger (Fig. 2 a), which complicates geologic and compositional studies of regions located at latitudes > 40° and prevents observations of the polar regions, which will be

completely in shadow. This situation is even worse with the new mission scenario (CReMA4.2b22_1) (Fig. 2 b).

c) UVS

UVS will observe Ganymede's surface in the extreme and far-ultraviolet wavelengths in the 55-210 nm range and will help identifying the composition and physical characteristics of non-H2O ice compounds and their association with Ganymede's surface features (Gladstone et al., 2013). At least 50% coverage by UV images with a spatial resolution ≤3 km and a spectral resolution ≤ 2 nm for wavelengths between 100 and 200 nm is anticipated. High spatial resolution observations (≤ 1 km; spectral resolution: ≤ 2 nm from 100 to 200 nm) will be acquired on the leading hemisphere, particularly on the sub-Jovian quadrant, with emphasis on the spectral differences and spectral slopes between geologic features and the surrounding areas. Medium spatial resolution (≤ 5 km/px) will be used to map asymmetries between the leading and trailing hemisphere of the satellite due to contamination by exogenic material.

d) SWI

SWI will measure the radio brightness temperature of Ganymede in two Far Infrared (FIR) bands (480-0.566 μm and 235-277 μm wavelengths) simultaneously with very high spectral resolving powers of 10^6-10^7 (Hartogh et al., 2013). It will close the gap between millimeter and infrared depth sensitivities and identify the chemical and physical properties of the icy surface such as thermal inertia, impurity content, and the size of the irregularities and small structures in the subsurface (Ilyushin and Hartogh, 2020). SWI will enable to correlate the thermophysical and electrical properties of the satellite surface and subsurface with atmospheric properties and geologic features and will thus determine the sources and sinks of Ganymede's thin atmospheres

and exospheres, such as sublimation, sputtering and any cryovolcanic activity. In addition, SWI measurements will unravel how Ganymede's surface interacts with the Jovian magnetosphere (de Kleer et al., 2021). All these science goals will be addressed progressively, starting with an extensive medium-to-long range monitoring campaign, consisting of daily observations of the surface and atmosphere emission of all the Galilean satellites during the Jupiter phase of the mission, to cover the leading and trailing hemispheres over all phase angles (Wirström et al., 2020). These observations will help to identify surface regions for more focused observations during the flybys. Finally, a nearly global surface and atmosphere coverage will be obtained for Ganymede with a spatial resolution of about 5 km (at 250 μm) and 10 km (at 500 μm) during the GCO5000 campaign.

e) GALA

GALA can be operated on day- and night-side from ranges smaller than about 1000 to 1300 km and thus will observe Ganymede during closest approaches at flybys and pericentre passages in the elliptical orbit phase (Hussmann et al., 2019; Hussmann et al., 2013). GALA will provide absolute topographic heights with respect to the Ganymede geoid on global, regional and local scales and surface roughness measurements down to a scale of 10s of meters. The albedo at the laser wavelength of 1064 nm will be obtained for every range of measurement. Combining stereo-data sets from JANUS with altimetry data provided by GALA will provide topography and digital terrain models that are essential for geologic studies.

f) RIME

The ice penetrating radar, RIME will be the first instrument able to acquire direct subsurface measurements of Ganymede (Bruzzone and Croci, 2019; Bruzzone et al., 2013). The measurements of the vertical properties of the subsurface acquired by RIME will be then integrated with the

vertical structure on and above the surface measured by GALA and JANUS. RIME will operate at 9 MHz, a frequency designed for achieving a maximum penetration depth of 9 km in pure H_2O ice with two bandwidths modes that result in high vertical resolution (maximum of 50 m in ice) or low vertical resolution (140 m in ice). However, to avoid the interference of the Jupiter radio emission, which can significantly decrease the signal-to-noise ratio (SNR), RIME will operate in active mode only on the anti-Jovian side of Ganymede (and Callisto), while passive radar observations are planned in the remaining range of longitudes in close flybys, whenever the altitude is < 1000 km.

g) J-MAG, RPWI, PEP

Furthermore, surface properties monitored by the remote sensing instruments (JANUS, MAJIS, UVS, SWI, GALA, RIME) will provide a surface (and sub-surface) context to the fields and particle investigations. Ganymede's surface is clearly divided between regions belonging to open and closed magnetic field lines respectively, indicating a division in the precipitation of energetic charged particles toward the surface. This difference will be addressed by the JUICE fields and particle instruments (J-MAG, RPWI, PEP) in addition to several other science objectives related to surface (and sub-surface) properties of Ganymede (Bergman et al., 2017; Dougherty and al., 2014; Wurz et al., 2018). Energetic particles (ions, electrons, neutrals, dust), monitored by the PEP and RPWI detectors, bombard the surface and change the composition and structure of the surface material. PEP will provide complementary information about weathering processes on Ganymede's and Callisto's surface (Vorburger et al., 2019) through sputtering and release of neutral and charged particles and unequivocal evidence for trace compounds formed by the interaction with the Jovian magnetosphere. PEP will also measure the local density and chemical

composition of the atmosphere along the JUICE trajectory. The magnetospheric source regions of the accelerating fields (electric potential structures or waves) will be monitored by RPWI and J-MAG, and the mechanism for the restructuring of the icy surface by the space environment can be found.

h) 3GM, PRIDE

The radio science experiment 3GM onboard JUICE has been primarily designed to determine the gravity field of Ganymede to degree and order 15 or higher through highly precise spacecraft tracking (Iess, 2013), which will enable the identification of density anomalies due to surface features and terrains (De Marchi et al., in revision) adding precious information on the correlation among surface and subsurface characteristics and density contrasts. In combination with GALA altimetry, this will determine the extent to which topography is expressed on the gravity field or is instead well compensated, the role of a silicate core, the possible role of convection, and the presence of regional differences in the outermost ice shell, which might allow to discriminate and separate the gravitational contributions from the deep interior and the surface distribution of dark and bright terrains (Fabrizio et al., 2021). In synergy with PRIDE's VLBI antennas (Gurvits et al., 2013), bistatic radar observations of Ganymede, which require specular reflection of the radio signal, in principle could enable to determine average surface slope, near-surface dielectric constant and, under certain assumptions, the surface porosity from the target scattering properties.

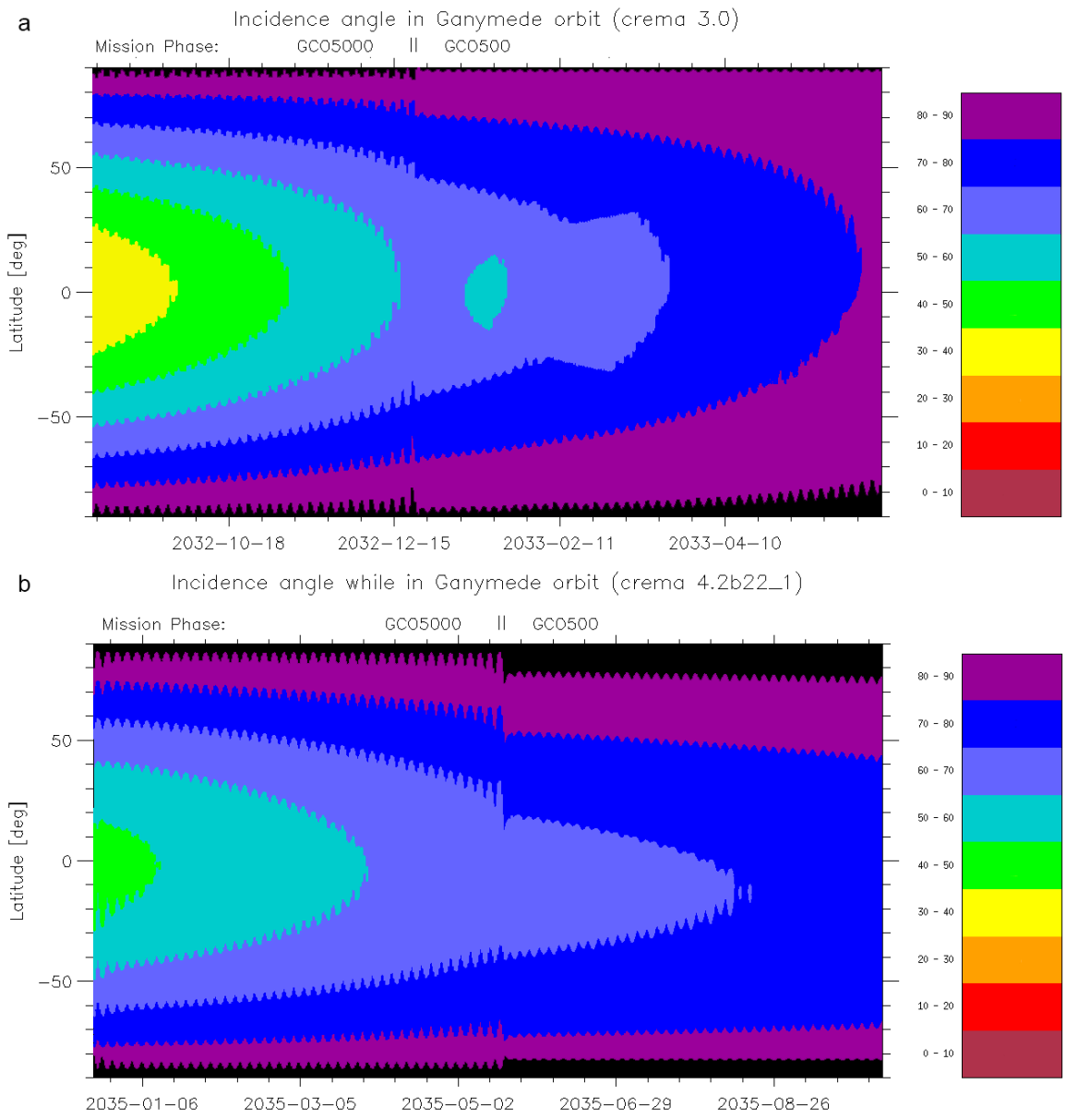

1

2 Figure 2: Development of the illumination conditions (incidence angle (°) during GCO5000 and
3 GCO500: a) based on CReMA 3.0 and b) CReMA 4.2b22.1 across the full range of latitudes on
4 Ganymede's surface.

2.2 Observation opportunities and possible coverage during GCO500 (and GCO200)

Because a nearly global coverage of Ganymede's surface by JANUS and MAJIS will be achieved in GCO5000, spatial resolutions of these imaging and spectral imaging data sets will provide the geologic and geomorphologic (3D reconstruction through stereo imaging) as well as compositional context for surface features, which will be imaged during GCO500 (and possibly during GCO200) at highest possible spatial resolution and will support the activities of all other JUICE instruments. Therefore, GCO500 will be dedicated to the characterization of regions of high interest (RoIs) for geology, chemistry, or physics with the highest level of detail. JANUS and MAJIS can achieve a nominal (unbinned) spatial resolution of ~7 m and ~ 74 m per pixel, respectively, with footprints too tiny to show up in a global map. JANUS will acquire colour data for up to three different filters. Depending on the local illumination conditions JANUS images acquired during GCO500 could be also useful for stereo imaging. During GCO500 the MAJIS scan mirror is mandatory and motion compensation is required which produces shorter along track images (14.1 km versus 30 km cross track size with a mean pixel size of 150 m). Both, JANUS and MAJIS, observations will take place only in a relatively small portion of the orbital time, due to the very high data production rate of both instruments. The instruments would be nadir pointed (emission angle = 0°), with no yaw steering during the JANUS and MAJIS observations. Outside of the JANUS and MAJIS observations the spacecraft would return to yaw steering mode, during which UVS would scan Ganymede for night-time aurora and daytime surface mapping with spatial resolution of about 500 m/pixel, and SWI would scan the surface under both daytime and night-time conditions with spatial resolution of about 500 m to study thermal inertia characteristics and perform atmospheric limb

scans to build 3D (latitude, longitude, altitude) atmospheric map as a function of time and illumination conditions.

GCO500 is indeed the prime mission for GALA, RIME and 3GM to address JUICE science objectives related to Ganymede's subsurface (including the ocean and the deep interior). GALA will have a ranging accuracy of less than one meter depending mainly on local surface slopes and albedo. The absolute topographic height error, however, will depend on the accuracy in the knowledge of the spacecraft orbit and attitude, and is expected to be a few meters. The spot diameter in GCO500 is about 50 m and GALA will be sensitive to surface roughness on these scales by measuring the broadening of the return pulse. In the nominal 30 Hz shot frequency mode the distance between the spot centres will be 50 m providing an excellent along-track resolution. Due to the polar orbit in GCO500 the surface coverage with ground-tracks is not homogeneous. As indicated before, while the coverage is densest at the poles and high latitude regions, there remain across-track gaps of several km in the equatorial regions. However, the along-track resolution which is independent of latitude provides essential characteristics of geologic features that are either axisymmetric in plan view or which have a predominant trend that is normal to the ground track. As mentioned above, RIME will preferably operate on Ganymede's anti-Jovian side (about 1/3 of the total surface) and some additional RoIs depending on limitations in downlink. Radio tracking by 3GM will operate during the downlink phase when the HGA is pointed towards the Earth (i.e., 8 hours per day). This will permit precise measurements of the moon's gravitational field via perturbations to the spacecraft orbit.

In addition, the plasma and fields instruments (J-MAG, RPWI and PEP) should operate continuously during the GCO500 phase to decipher the complex combination of the fields (Jovian, intrinsic and induced fields). Furthermore, certain regions of interest, such as the auroral latitudes

at Ganymede or the polar region, are of particular interest and detailed planning is required for each orbit. Particularly, PEP provides imaging of the precipitating particles in backscattered ENAs to identify correlations with changes in the spectral surface signature due to surface weathering operating semi-continuously with the focus on the polar regions inside the open/close field line boundary (> 50° latitude).

In the framework of a potential Extended Mission of the Ganymede orbit (Tab. 1), a Low Altitude Orbit with an altitude of ~200 km above the surface (GCO200) could be performed if resources allow it at the end of GCO500. For remote sensing instruments with imaging capabilities, this phase would be affected by substantial smearing due to the very fast movement of the ground footprint compared to the exposure time required to achieve a sufficient SNR, plus long shadows in the observed scene, which ultimately would result in an extremely low data quality. However, although a GCO200 phase is far from being optimal for UV to IR remote sensing, it is optimal for the entire scope of the mission. This phase was particularly longed for as it would be essential for in situ measurements and geophysical experiments such as RIME, PEP, RPWI and JMAG, which will be also crucial for the understanding of the geologic and compositional surface processes.

2.3 Callisto flybys

The coverage of Callisto by the imaging and spectral imaging JUICE instruments is constrained by the number of flybys and by the geometric circumstances of those flybys, which actually strongly change from one mission profile to another, resulting in a variable degree of redundancy. The most detailed studied mission profile CReMA 3.0 indicated that large portions of Callisto's anti-Jovian hemisphere and parts of the sub-Jovian hemisphere can be observed during these flybys with the

best spatial resolution close to the equator (Fig. 3 - 5). Observations at highest possible spatial resolutions by JANUS and MAJIS are limited (Fig. 3 a and 4). Only observations at low and medium spatial resolutions overlap to a significant amount offering either opportunities of JANUS stereo imaging and/or possibilities to reduce the number of JANUS and MAJIS observations due to possible data volume constraints (Fig. 5).

Based on the mission scenario (CReMA 4.2b22.1), JUICE may experience up to 19 Callisto flybys during the Jupiter tour, which would significantly increase the coverage of Callisto at a regional scale. Coverage at high spatial resolution would also be improved. Even more, the increased number of ground tracks would improve topographic models, ionospheric and exospheric models, global shape measurements, gravity field determinations and measurement of the tidal deformation. Time variability of the exospheric properties, which has to do with the illumination angle and with the arrival detection of the plasma flow, would be better constrained (Vorburger et al., 2019).

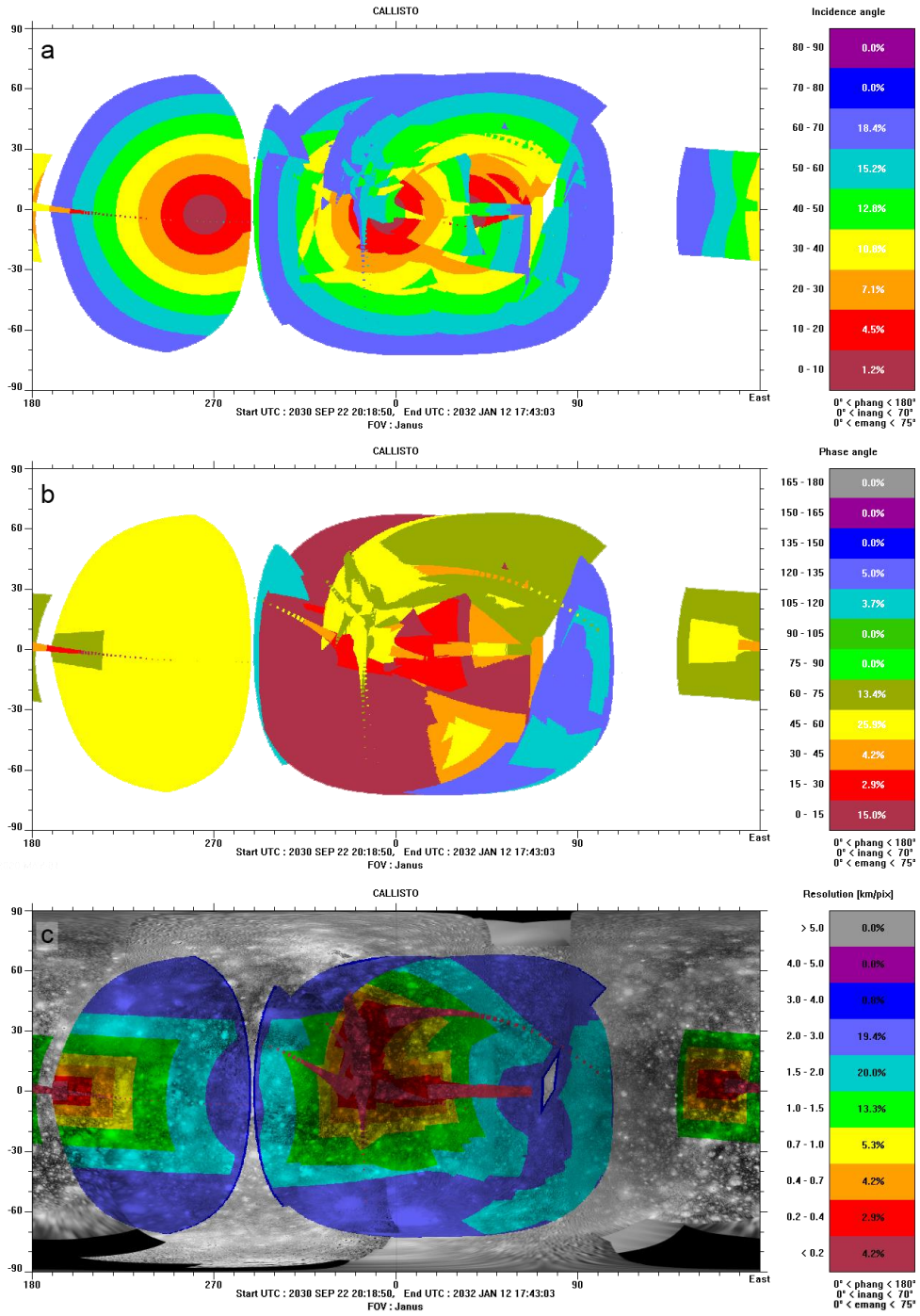

1

2 Figure 3: JANUS coverage (nadir-looking only) during the Callisto flybys (CReMA 3.0): a)
3 incidence angle, b) phase angle and c) spatial resolution overlaid onto the global Galileo/Voyager
4 base map provided by USGS.

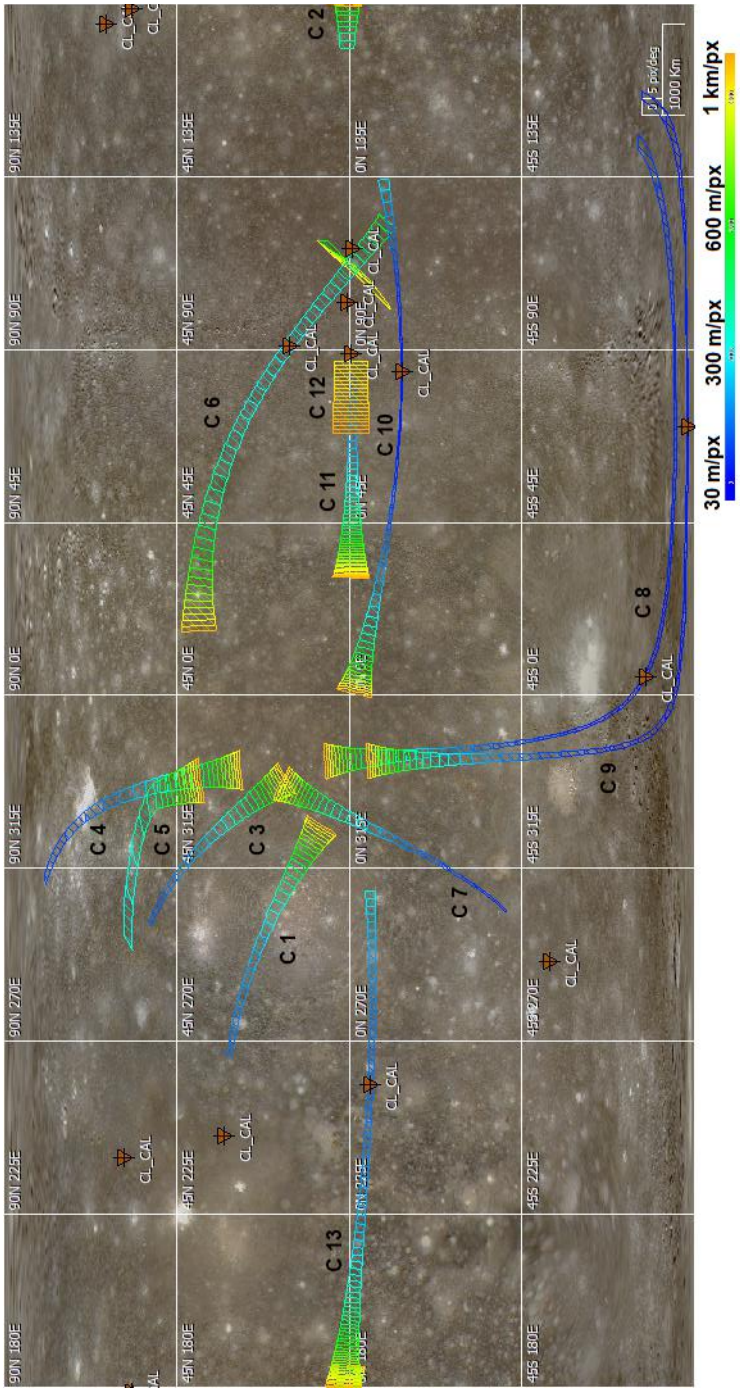

Figure 4: MAJIS coverage by observation with spatial resolution better than 1 km / pixel during the Callisto flybys (CReMA 3.0). Please note that no significant overlap exists among the flybys. The Figure was prepared using the Mission Analysis and Payload Planning System (MAPPS) of ESA (Van Der Plas and Nespoli, 2016).

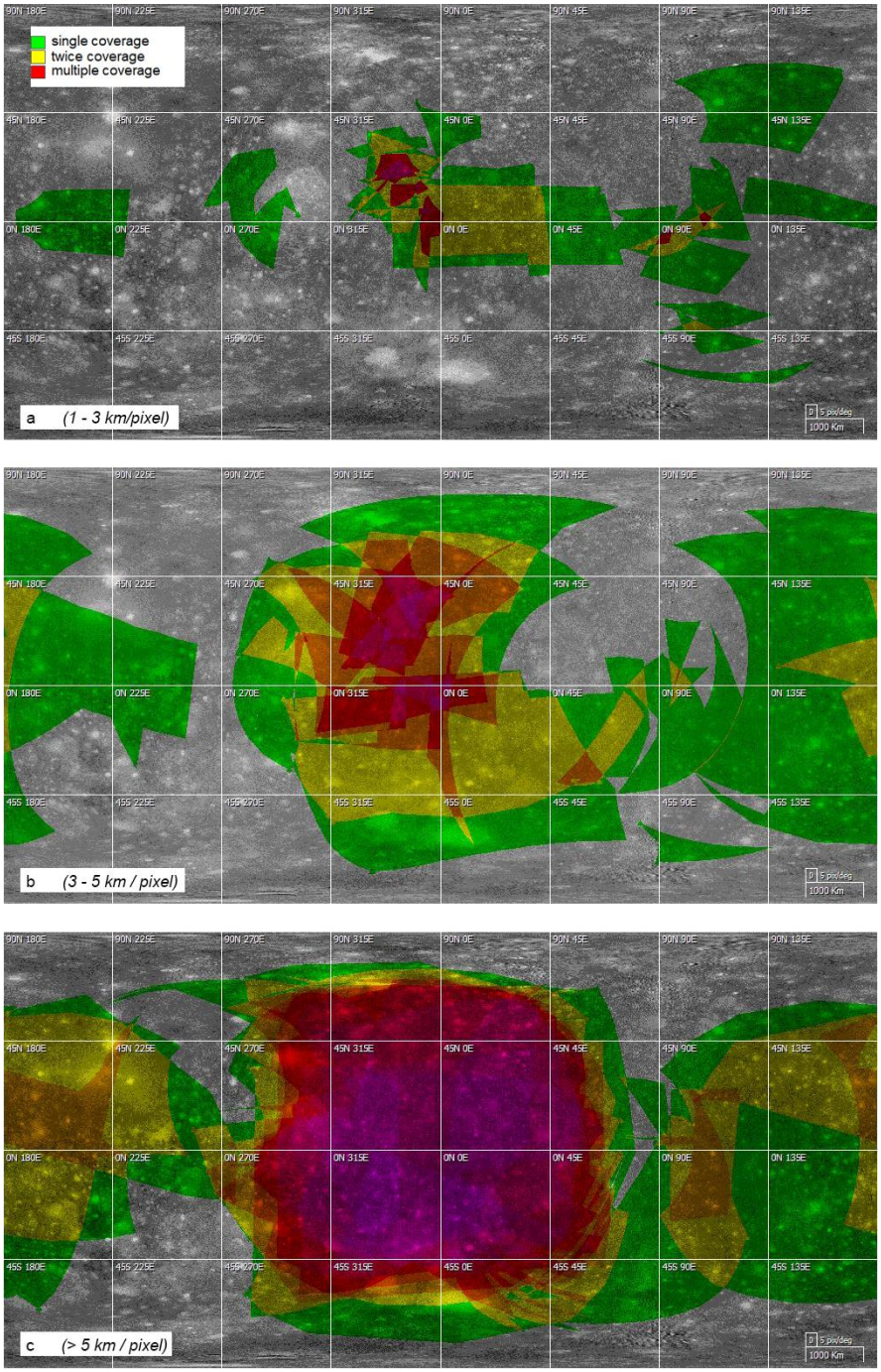

Figure 5: MAJIS coverage during the Callisto flybys (CReMA 3.0) by observations with spatial resolutions a) between 1 and 3 km / pixel, b) 3 and 5 km / pixel and c) > 5 km / pixel with the overlap of MAJIS observations indicated. The Figure was prepared using the Mission Analysis and Payload Planning System (MAPPS) of ESA (Van Der Plas and Nespoli, 2016).

3 RoI selection (Motivation and Procedure)

The planning activities of the JUICE SWT and scientific WGs concerning Ganymede and Callisto imply 1) discussions on the potential outcome of different flyby geometries, 2) the preparation of observational strategies for each instrument, 3) the understanding the opportunities for synergistic observations between instruments, 4) the discussions in terms of pointing, power, time allocation, data volume, etc. These activities, all dealt with in order to optimize the scientific return of the different mission phases, require the development of a common tool and/or guidelines such as a selection of high priority RoIs on the surfaces of Ganymede and Callisto, which present key features that are essential to understand Ganymede's and Callisto's evolution. This selection of RoIs is particularly required with respect to the low orbit phases at Ganymede (GCO500 and GCO200) and the Callisto flybys. Nevertheless, as stated above, because the mission time line and number of flybys at Callisto can still significantly change, the RoIs are crucial for the instrument teams to prepare at best their observation strategies whatever the orbit and flyby geometries. Therefore, the RoIs proposed in this work span across the entire surface of both bodies and can be adapted in the future by the JUICE SWT, and WGs and each instrument team for their specific observation requirements.

We have selected the proposed RoIs based on the coverage of the Ganymede and Callisto surfaces available from Voyager and Galileo imaging data, and on the most recent geologic map of Ganymede (Collins et al., 2013; Patterson et al., 2010). Our list of RoIs thus represent surface features and areas that have already been imaged, at least partly. However, spatial resolutions were generally too low to study them in detail and complementary information about their geologic age,

surface composition, surface and subsurface properties, topography and radiation environment and orbital properties, which is needed to resolve their nature, are either rare or non-existent at all. Therefore, in addition to their importance from a geologic and compositional point of view RoIs have been selected with respect to their possible relationships to Ganymede's and Callisto's exospheres, temperature and radiation environments, subsurface properties, and also to their orbital evolution and influences due to Ganymede's magnetic field. This synergy is essential for the investigation of Ganymede as a planetary object and possible habitat and Callisto as a remnant of the early Jovian system according to the major JUICE Science objectives (ESA JUICE definition study report /Red Book, ESA/SRE(2014)):

Ganymede Objectives (G): ***Characterize Ganymede as a planetary object and possible habitat***

- GA) The ocean and its relation to the deep interior
- GB) Characterization of the ice shell
- GC) Local environment and its interaction with the Jovian magnetosphere
- GD) Formation of surface features and search for past and present activity
- GE) Global composition, distribution and evolution of surface materials

Callisto Objectives (C): ***Callisto as a remnant of the early Jovian system***

- CA) Characterize the outer shell, including the ocean
- CB) Determine composition of the non-ice material
- CC) Study of the past activity

Depending on the geomorphologic characteristics, stratigraphic position (= geologic age), chemical and physical surface properties of the proposed RoIs, the possible formation processes including their relationship to the bodies' internal processes/structure or interaction with the external environment the selected RoIs can be organized into seven categories (Fig. 6). Because of the large similarities in the morphology of the surface terrains and features as well as possible formation processes (although under different environmental conditions), the categories defined for Ganymede have been similarly applied for Callisto.

Although, all categories and their associated RoIs are of equally high scientific importance, the opportunities to study them during the JUICE mission depend on their abundance and distribution across Ganymede's and Callisto's surfaces and possible limitations of their observability by some of the JUICE instruments at the given illumination conditions during the mission. Therefore, we have given each category a priority to ensure that a sufficient number of RoIs of all categories will be investigated. Consequently, a specific category, whose RoIs, based on the recently known illumination conditions of the JUICE mission, can be only observed at the beginning of the JUICE mission, or that consist of only a few local surface features, which require imaging at highest spatial resolution combined with special orbit and flyby geometries, have been given a higher priority than priorities assigned to other categories, which consists of more frequent and equally distributed RoIs on both bodies, and whose observation is not restricted by any flyby and/or orbit and observation requirements.

The distribution of the selected RoIs across Ganymede's and Callisto's surface are presented in Figures 7 and 8 (the maps showing the RoIs separately for each category can be found in the supplementary material) and listed in Table 3 and 4. Each category is indicated by a different colour in the maps and the RoI lists. An identification number (ID) is given to each proposed RoI, which

corresponds to the category and its position in the RoI list of the corresponding category. For each RoI, the name (if existing) of the major surface feature, its geographic location and its size are listed, followed by the dimensions of the area that covers the entire surface feature/region. The scientific rationale follows the general description of each specific RoI. The document includes a suggestion about which JUICE instruments are mandatory to complementary investigate the proposed targets. Next to remote sensing instruments covering a broad spectral range from the ultraviolet to the microwaves such as JANUS, MAJIS, UVS, SWI, also GALA and RIME as well as PEP, RPWI, J-MAG and 3GM are included, because of the close relationship of surface properties to the subsurface and interior as well as the atmosphere, the space environment (temperature, radiation, magnetic field) and orbital parameters. In the following, each category will be discussed in detail with respect to their association with the individual JUICE science objectives and which science questions can be investigated during the different mission phases (Fig. 6).

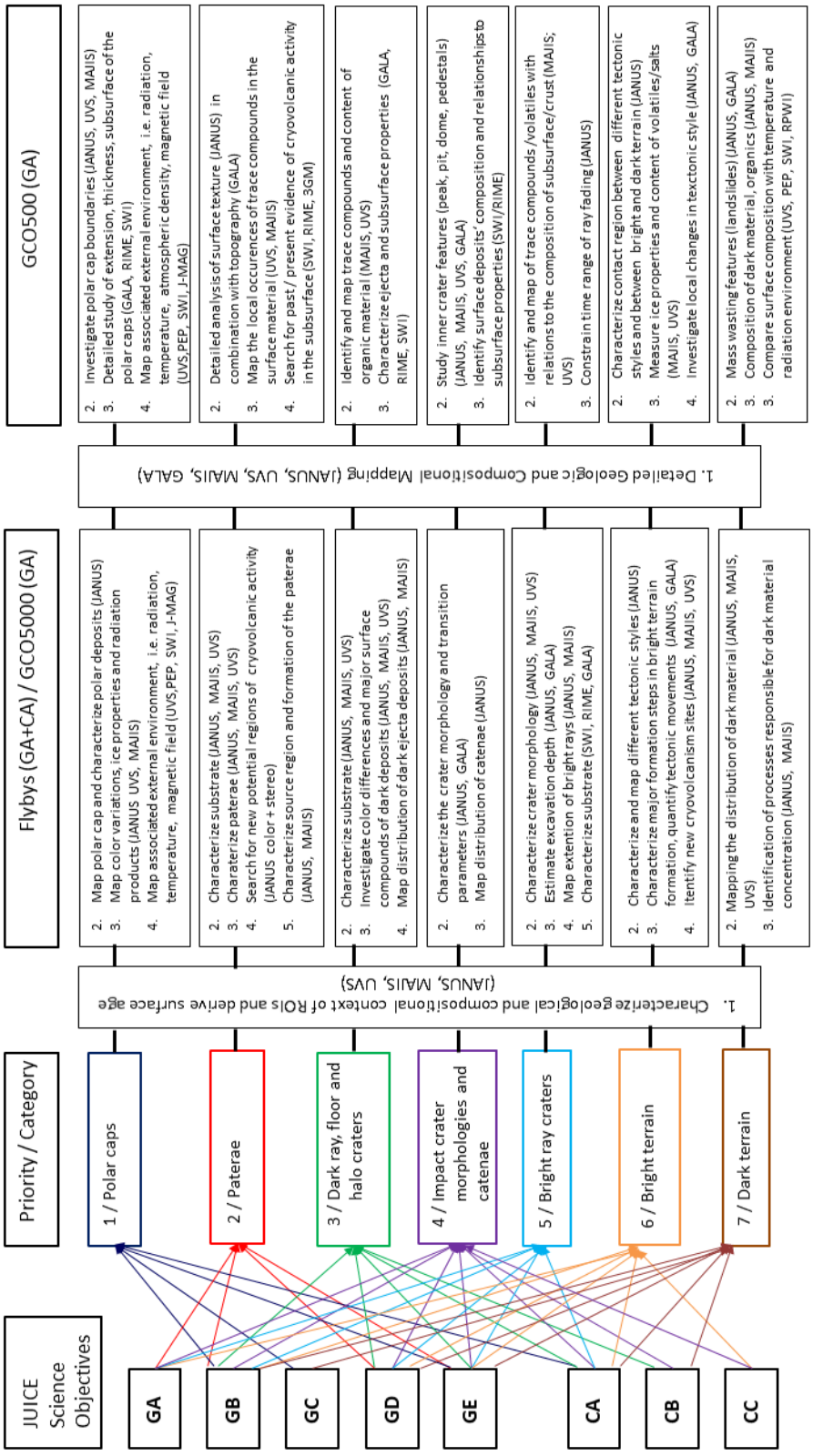
JUICE Science Objectives
Priority / Category
Flybys (GA+CA) / GCO5000 (GA)
GCO500 (GA)
GA
GB
GC
GD
GE
CA
CB
CC
1 / Polar caps
2 / Paterae
3 / Dark ray, floor and halo craters
4 / Impact crater morphologies and catenae
5 / Bright ray craters
6 / Bright terrain
7 / Dark terrain
1. Characterize geological and compositional context of ROIs and derive surface age (JANUS, MAIS, UVS)
1. Detailed Geologic and Compositional Mapping (JANUS, UVS, MAIS, GALA)
2. Map polar cap and characterize polar deposits (JANUS)
3. Map color variations, ice properties and radiation products (JANUS UVS, MAIS)
4. Map associated external environment, i.e. radiation, temperature, magnetic field (UVS,PEP, SWI, J-MAG)
2. Investigate polar cap boundaries (JANUS, UVS, MAIS)
3. Detailed study of extension, thickness, subsurface of the polar caps (GALA, RIME, SWI)
4. Map associated external environment, i.e. radiation, temperature, atmospheric density, magnetic field (UVS,PEP, SWI, J-MAG)
2. Characterize substrate (JANUS, MAIS, UVS)
3. Characterize paterae (JANUS, MAIS, UVS)
4. Search for new potential regions of cryovolcanic activity (JANUS color + stereo)
5. Characterize source region and formation of the paterae (JANUS, MAIS)
2. Detailed analysis of surface texture (JANUS) in combination with topography (GALA)
3. Map the local occurences of trace compounds in the surface material (UVS, MAIS)
4. Search for past / present evidence of cryovolcanic activity in the subsurface (SWI, RIME, 3GM)
2. Characterize substrate (JANUS, MAIS, UVS)
3. Investigate color differences and major surface compounds of dark deposits (JANUS, MAIS, UVS)
4. Map distribution of dark ejecta deposits (JANUS, MAIS)
2. Identify and map trace compounds and content of organic material (MAIS, UVS)
3. Characterize ejecta and subsurface properties (GALA, RIME, SWI)
2. Characterize the crater morphology and transition parameters (JANUS, GALA)
3. Map distribution of catenae (JANUS)
2. Study inner crater features (peak, pit, dome, pedestals) (JANUS, MAIS, UVS, GALA)
3. Identify surface deposits' composition and relationships to subsurface properties (SWI/RIME)
2. Characterize crater morphology (JANUS, MAIS, UVS)
3. Estimate excavation depth (JANUS, GALA)
4. Map extention of bright rays (JANUS, MAIS)
5. Characterize substrate (SWI, RIME, GALA)
2. Identify and map of trace compounds /volatiles with relations to the composition of subsurface/crust (MAIS; UVS)
3. Constrain time range of ray fading (JANUS)
2. Characterize and map different tectonic styles (JANUS)
3. Characterize major formation steps in bright terrain formation, quantify tectonic movements (JANUS, GALA)
4. Itentify new cryovolcanism sites (JANUS, MAIS, UVS)
2. Characterize contact region between different tectonic styles and between bright and dark terrain (JANUS)
3. Measure ice properties and content of volatiles/salts (MAIS, UVS)
4. Investigate local changes in texctonic style (JANUS, GALA)
2. Mapping the distribution of dark material (JANUS, MAIS, UVS)
3. Identification of processes responsible for dark material concentration (JANUS, MAIS)
2. Mass wasting features (landslides) (JANUS, GALA)
3. Composition of dark material, organics (JANUS, MAIS)
3. Compare surface composition with temperature and radiation environment (UVS, PEP, SWI, RPWI)

1

Figure 6: Scheme of the JUICE science objectives related to the categories of the proposed Regions of Interest (RoI) and the key science questions, which should be focused on during the different JUICE mission phases (flybys, GCO5000 and GCO500). Please note that for Callisto only the comments relative to the flybys are relevant for Callisto.

>>Table 3: List of proposed regions of interest (RoIs) for Ganymede.

>>Table 4: List of proposed regions of interest (RoIs) for Callisto.

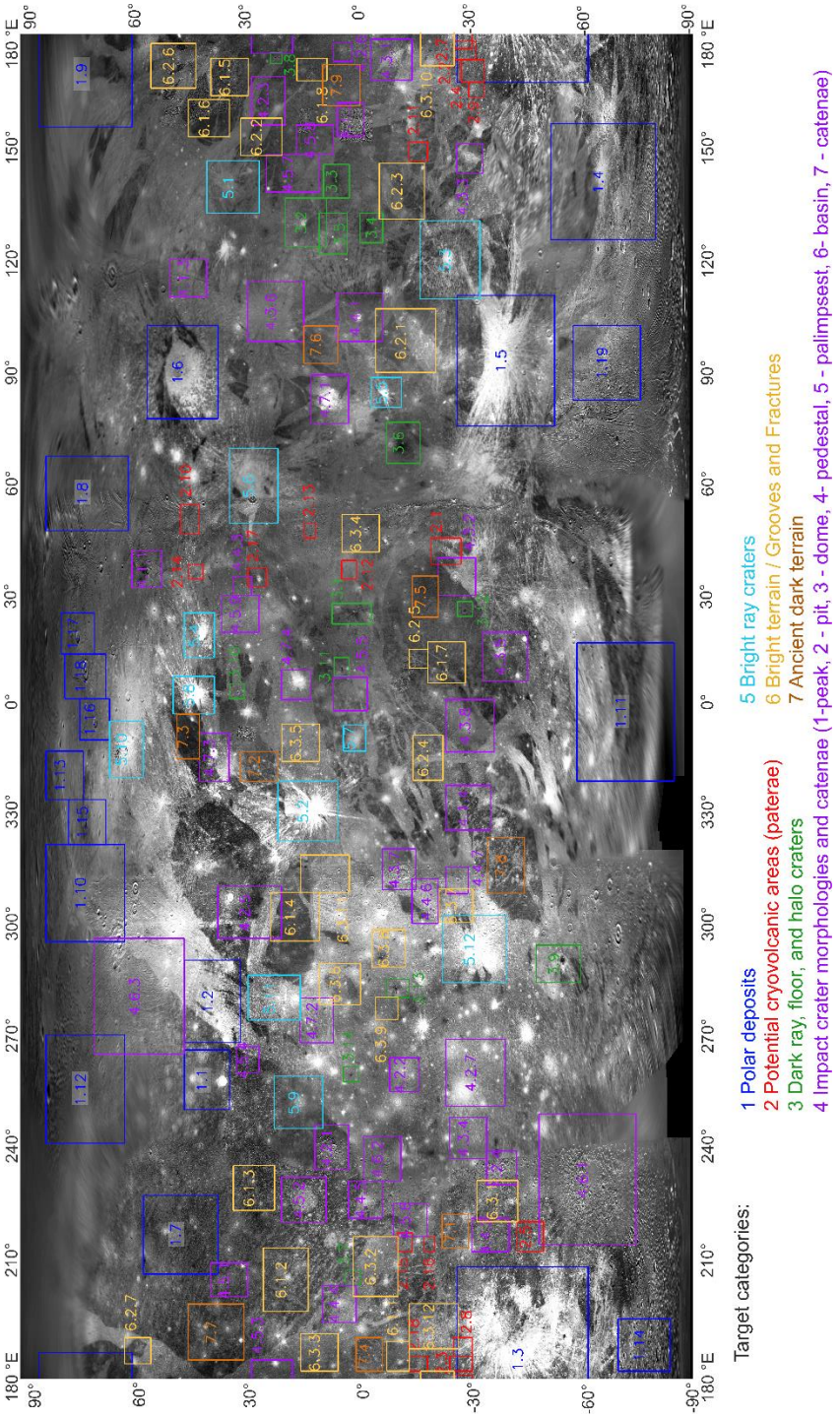

Figure 7: Location of the proposed regions of interest (RoIs) for Ganymede overlaid onto a global Galileo Solid-State Imaging (SSI)/Voyager Imaging Science Subsystem (ISS) image mosaic. Please see the maps separately for each category in the supplementary material (Figs. SM 1 to 7).

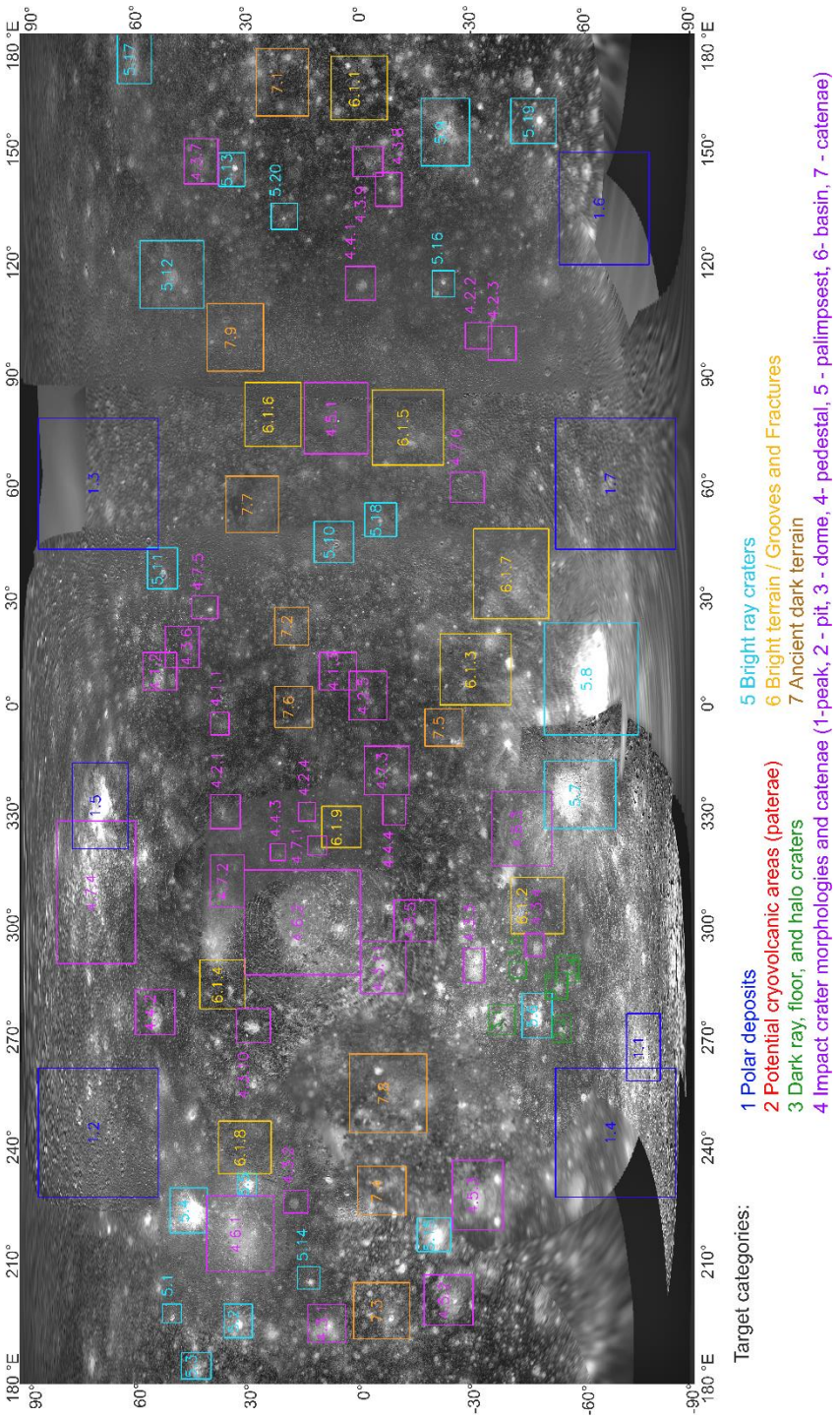

Figure 8: Location of the proposed regions of interest (RoIs) for Callisto overlaid onto a global Galileo Solid State Imaging (SSI)/Voyager Imaging Science Subsystem (ISS) mosaic (Maps of the

RoIs separately for each category are provided separately in the supplementary material). Please see the maps separately for each category in the supplementary material (Figs. SM 8 to 13).

4 RoI Categories

4.1 Polar deposits

Ganymede's polar caps are a thin veneer of polar frost deposits (Smith et al., 1979) that depending on its thickness more or less completely masks the spectral signature and morphological characteristics of the underlying terrain (Fig. 9 a). These deposits are supposed to be a direct result of a complex mixture of exogenic surfaces processes reaching from the unique interaction with the Jovian magnetosphere (Johnson, 1997; Johnson et al., 2007; Khurana et al., 2007) and the thermal environment (Spencer, 1987; Squyres, 1980; Stephan et al., 2020). Since, Ganymede as well as Callisto orbit Jupiter within the planet's magnetosphere with the impacting radiation greatly affecting the chemical and physical surface properties of the satellites (Paranicas et al., 2018), the characterization of the interaction between the satellites' icy surface, the local environment and the Jovian magnetosphere is one of the top science objectives (GB/GC/GE and CA) of the JUICE mission. Because of the different orbital distances of Ganymede and Callisto from Jupiter, the interaction differs in strength and configuration. At Ganymede, this interaction is even more complex due to the existence and configuration of Ganymede's own magnetic field (Kivelson et al., 1996), which partly shields the equatorial region between ±40° latitude from impacting plasma where competing processes such as thermal migration and micro-meteoritic bombardment become more dominant.

The synergy of both, the remote sensing and geophysical JUICE instruments, is necessary to solve the mystery of Ganymede's polar caps and to rule out competing surface processes such as thermal migration as a source for Ganymede's polar deposits. Based on the recent knowledge about the configuration of the magnetic field and the variations in the precipitation of plasma onto Ganymede's surface as described by Fatemi et al. (2016), we defined RoIs throughout Ganymede's Southern and Northern polar caps, i.e. from mid-latitudes, where the polar deposits become apparent in the SSI images and Ganymede's magnetic field lines change from closed to open ones (Fig. 7, Tab. 3), to higher latitudes, to compare regions of pronounced and low plasma precipitation. We defined RoIs on Callisto at similar locations as on Ganymede (Fig. 8, Tab. 4) to use the unique opportunity to observe two bodies, which both orbit Jupiter within its extensive magnetosphere, and therefore to study differences in the moon-plasma interaction depending on the distance of the satellites from Jupiter.

It has to be noted, however, that the observation of Ganymede's poles by the imaging and spectral imaging instruments can only be performed in GCO5000 due to the increasingly unfavourable illumination conditions at Ganymede's high latitudes with the evolution of the orbital phase (Fig. 2). Although, JUICE instruments are partly independent of the illumination conditions and can perform measurements on the nightside or in shadowed areas (atmospheric studies by UVS, SWI, RIME), complementary information of the polar surface properties from JANUS, MAJIS and UVS are necessary to interpret the scientific data in detail. In addition, the coverage of GALA will be best in both polar regions and also requires geologic context information. Therefore, it is highly recommended to perform observations of Ganymede's surface at its poles by JANUS, MAJIS and UVS as early as possible, i.e. at the beginning of GCO5000. We assigned the highest priority (1)

to this category to highlight this requirement to enable high resolution imaging and spectral imaging context information in the polar regions of Ganymede.

During GCO5000 JANUS, images of the polar regions with a spatial resolution of at least 70 m/pixel, an incidence angle < 70° and higher sensitivity of the JUICE imaging and spectral imaging instruments could reach a quality close to or better than the best-resolved Galileo SSI images located in the polar caps (Fig. 9 a). Imaging and spectral imaging data will reveal the extent of the polar caps on Ganymede and directly identify and map radiation effects in the surface material. From MAJIS' hyperspectral imaging data, differences in the crystallinity and particle sizes of H_2O together with radiation products implanted or formed within the surface material such as O_2, O_3, H_2O_2, H_2SO_4 or possible more complex hydrocarbons (Delitsky and Lane, 1998; Hansen and McCord, 2004; Johnson et al., 2007) can provide a detailed view into the radiation-induced chemistry. Any time variability of the distribution of these surface properties can be related to the actual configuration of the magnetic field (J-MAG), i.e. the location of the boundary between open and closed magnetic field lines, the local plasma precipitation and atmospheric density (PEP), and the activity of Ganymede's aurora (UVS). Surface temperatures and atmospheric properties derived by SWI could help to distinguish the competing processes due to radiation and temperature variations.

As the illumination conditions become worse during GCO5000 and GCO500 and even worse for the new mission schedule, Ganymede's surface at latitudes higher than ~50° would be dominated by shadows (with the imaging and spectral imaging data easily affected by artefacts of overexposed areas due to the high contrast between dark and very bright illuminated icy regions (Fig. 9 b) or are completely hidden in the dark (Fig. 2). Possibly, early in GCO500 imaging and spectral imaging observations of RoIs at mid-latitudes may still be possible to some degree and allow monitoring

the polar caps boundaries in combination with the location of the transition from closed to open magnetic field lines, the variations in the plasma precipitation as well as atmospheric conditions (including Ganymede's aurora) derived by PEP and J-MAG and UVS, respectively (Fig. 2). UVS will also continue to monitor less illuminated regions including Ganymede's night side in GCO500 via observations of reflected interplanetary lyman alpha and FUV starlight to search for condensed volatiles and increased porosity, as demonstrated by the similar LRO-LAMP instrument for the Lunar permanently shadowed regions (Gladstone et al., 2012). GALA and RIME will help to constrain the thickness and age of the polar caps and thus possibly indirect information about the age of Ganymede's magnetic field, as well as together with JANUS imaging data how the polar ice deposits influence the local surface properties including the surface features and terrain types discussed below, which is essential to keep in mind, when investigating their morphology, composition, geologic age, physical and chemical weathering effects.

The relatively large size of the selected RoIs in this category have been chosen with respect to the different resolution capabilities of the different JUICE instruments. However, in case of data volume constraints with respect to high-resolution imaging and spectral imaging data by JANUS and MAJIS in GCO500, it might be possible that the RoIs cannot be observed entirely. In this case a set of observations displaying the N-S oriented transition to/from the polar caps across Ganymede's surface (Fig, 7 d) might be the best strategy to get an idea how the polar caps evolve depending on latitude and across the local terrain. In combination with the observations of individual surface features and terrain types discussed in the next sections, these data will strengthen our knowledge about how the polar deposits affect the surface characteristics of these features, which is essential, when investigating their formation processes and constraining compositional input parameters for experimental studies.

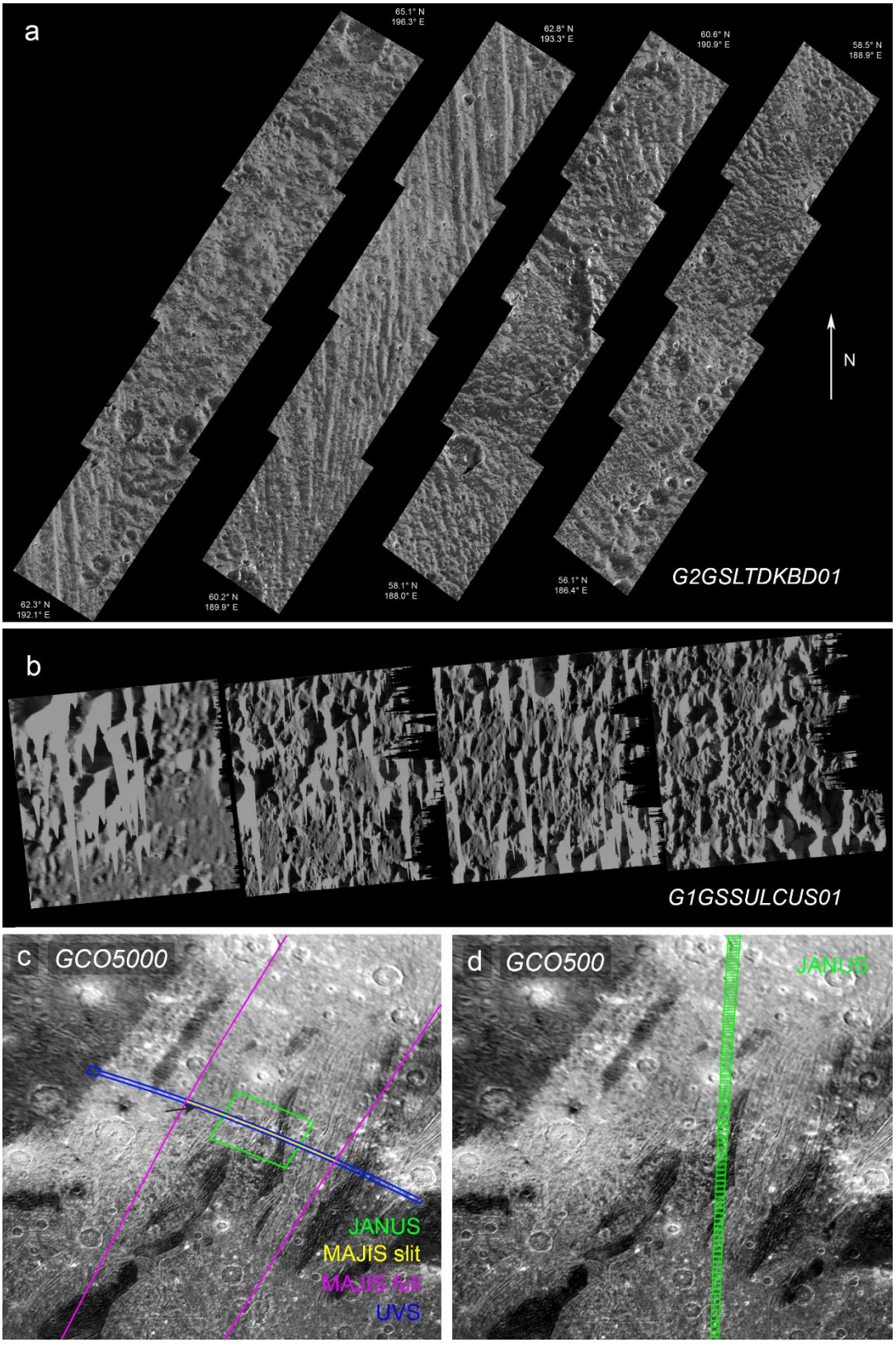
a
65.1° N
196.3° E
62.8° N
193.3° E
60.6° N
190.9° E
58.5° N
188.9° E
N
G2GSLTDKBD01
62.3° N
192.1° E
60.2° N
189.9° E
58.1° N
188.0° E
56.1° N
186.4° E
b
G1GSSULCUS01
c GCO5000
JANUS
MAJIS slit
MAJIS full
UVS
d GCO500
JANUS

1

Figure 9: Ganymede's polar caps: a) best resolved Galileo SSI mosaic from G2GSLTDKBD01 (i=~64°, e=~61°, p=~33°, map scale = 46m/pixel), b) Galileo SSI images from G1GSSULCUS01 dominated by artefacts due to high incidence angle and high brightness variations: (~30°N/269°E, i= ~ 83°, e = ~7°, p= ~79°, map scale=10m/pixel), c) RoI #1.2 showing the transition to the polar caps in Xibalba Sulcus (36°N/280°E) overlaid by the IFOV of JANUS, MAJIS and UVS during GCO5000 and d) a set of GCO500 JANUS observations enabling the detailed observation of the transition to the polar caps at open/closed field lines boundary.

4.2 Potential cryovolcanic regions

The investigation of past and/or recent geologic activity and its relation to the shallow subsurface and possible interaction with an ocean is one of the top priorities of the JUICE mission (GA/GB/GD/GE and CA/CC) to characterise the conditions that may have led to the emergence of habitable environments among the Jovian icy satellites (Grasset et al., 2013). Already during the Voyager and Galileo mission signs of possible past cryovolcanic activity could be observed in a few isolated spots on Ganymede's surface. These spots were described as "scalloped depressions" ("*paterae*") (Fig. 10) and interpreted as possible caldera-like source vents for icy volcanism (Kay and Head, 1999; Lucchitta, 1980; Schenk et al., 2001; Schenk and Moore, 1995; Spaun et al., 2001). However, most of these paterae have not been observed with sufficient spatial resolution by imaging instruments and no complementary information about the local topography, surface age and composition has been acquired yet preventing to find unequivocal evidence for their cryovolcanic nature, a possible interaction with Ganymede's subsurface ocean and relationships to the satellite's habitability. Consequently, previously identified spots included in the geologic map of Collins et al. (2013) have been re-selected as potential RoIs for the JUICE mission.

On Callisto, no evidence of past or present subsurface processes such as cryovolcanism have been identified so far. Areas of smooth terrain that have been suspected after Voyager as cryovolcanic resurfacing rather represent thick lag deposits of dark non-ice material created by sublimation as seen in spatially higher resolved Galileo images (Moore et al., 2004). Therefore, no RoIs have been defined for Callisto in this category. Specific observation planning is required to observe these rare and mostly very local, small-scaled surface features by the JUICE instruments and to enable the synergetic observation of these surface features by the JUICE instruments. Therefore, priority 2 has been assigned to this RoI category.

Synergy between highest-resolution imaging and spectral imaging (JANUS, UVS, MAJIS, SWI) together with laser altimetry (GALA) and subsurface radar (RIME) is mandatory to reveal the origin and formation of Ganymede's paterae. The dimensions of these paterae do not exceed ~20 km by ~70 km (Tab. 3) and can be more or less covered during the Ganymede Flybys and GCO5000 with a single JANUS, MAJIS and UVS observation (Fig. 11). The imaging and spectral imaging data will provide the geologic and compositional context, i.e. 1) which terrain types are associated with the occurrence of the paterae, 2) when the paterae have been emplaced and 3) if surface compounds other than H_2O ice can be already identified in the spectral data set of UVS and MAJIS. The images can already help to get an idea of how these paterae evolved. These ideas can be verified during GCO500 (Fig. 11 b) using a detailed mapping of the paterae including the surface texture and their geologic contact to the surrounding terrain types based on the combination of JANUS images and topographic information (JANUS stereo imaging and GALA). MAJIS' ability to map the surface composition of potential cryovolcanic features at the local scale (~75 m/pixel) during GCO500 with a spectral sampling between ~ 4 nm (VIS-NIR) and ~ 7 nm (IR) and a sufficient SNR (Langevin and Piccioni, 2017; Piccioni et al., 2019), is essential for quantifying the

local H_2O ice properties (crystallinity, particle size) and identifying and mapping the narrow absorptions of compounds such as salts, volatiles and organics (Ligier et al., 2019) that could be remnants of extrusion of liquids from the subsurface in a relatively recent past. Thus, this high-resolution imaging and spectral imaging data set, will enable to characterize the formation process in detail. In case of relatively young paterae complementary information by SWI and RIME about possible temperature variations, the determination of the minimal thickness of Ganymede's icy crust at this location, the detection of buried older terrain mantled by cryo-lava (Thakur and Bruzzone, 2020; Thakur and Bruzzone, 2021) and possible associated liquid pockets in the shallow subsurface could reveal unequivocal evidence for cryovolcanic processes with interaction to Ganymede's subsurface ocean. In addition, SWI will be able to detect any on-going cryovolcanic plumes and constrain their composition (H_2O and other trace species such as CO, HCN, NH_3, KCl, NaCl, etc.), as it is a link to the surface and subsurface material.

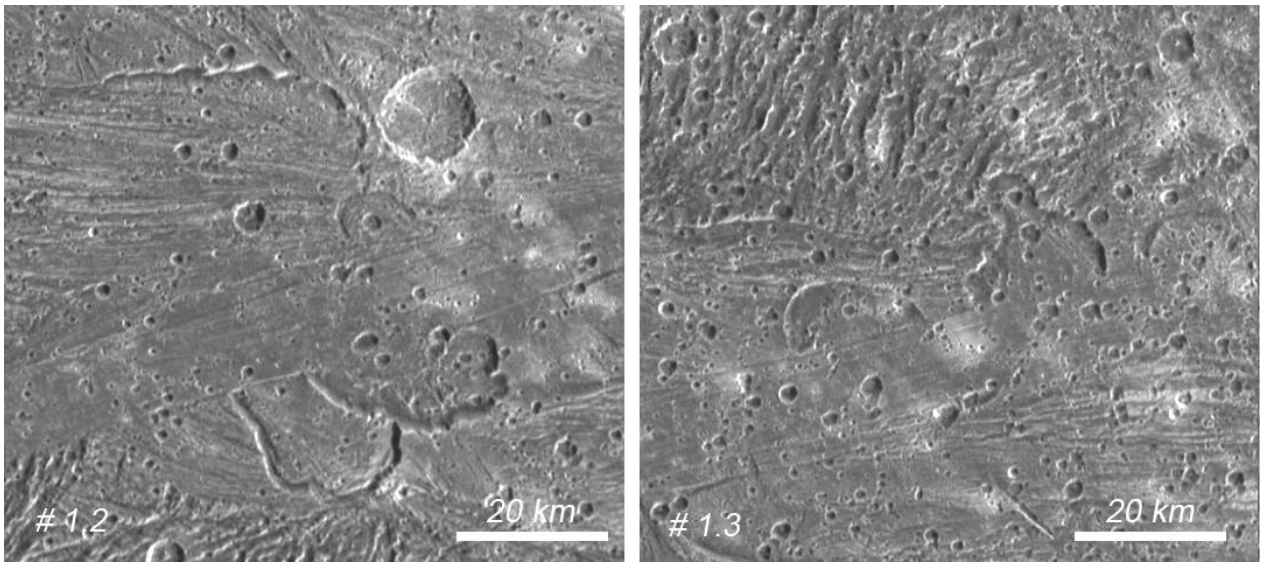

Figure 10: Examples of the best resolved paterae (~180 m per pixel) on Ganymede: (left) Natrum/Rum (30.8°S/177°E) and (right) unnamed patera (30.9°S/176.7°E) observed by Galileo

SSI (G8GCCALDRA01), which have been incorporated in the list of potential RoIs with the ID#2.2 and #2.3, respectively.

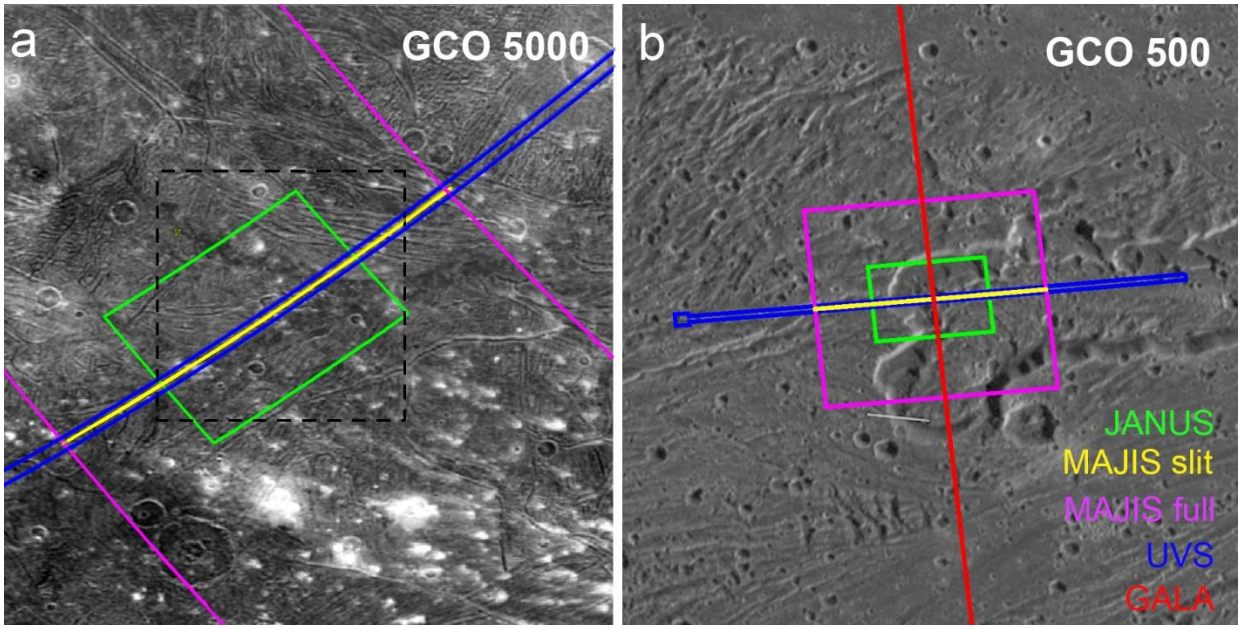

Figure 11: Footprints of different JUICE instruments (JANUS (green), MAJIS FOV built over time (magenta), MAJIS single slit pointed at boresight (yellow), UVS (blue), GALA (red) during a) GCO5000 and b) GCO500 for Musa Patera located at 31.4°S/171.5°E (RoI #2.4, 69 km) (please note that the GCO5000 footprints are larger than the defined RoI that is indicated by the dashed line). Please note that GALA will not operate during GCO5000.

4.3 Dark Ray, Floor and Halo Craters

Some of Ganymede's most peculiar surface features are impact craters with dark deposits (Fig. 12) such as (1) bright ice-rich craters with dark extended rays, (2) craters with a dark crater floor and presumably dark ejecta and (3) dark floored craters with a dark and/or a bright halo. These deposits

often represent the highest concentration of dark non-ice material(s) on Ganymede's surface (Hibbitts et al., 2003a; Schenk and McKinnon, 1991). The nature of these dark crater materials is still far from being understood. Available imaging and spectral imaging data are rare or poorly resolved since most of these impact features are very small (with diameters less than 10 km). In addition, information about their geologic context (substrate) is still missing, limiting the possibilities to study the origin and/or the formation of the dark compounds. Either the color diversity of the dark deposits resembles residuals of different types of impactors (Hibbitts et al., 2003b; Schenk and McKinnon, 1991) or is due to differences in the physical ice properties in combination with re-excavated portions of Ganymede's dark terrain (Stephan, 2006).

The investigation of these concentrated dark material deposits is a key area to resolve the composition and origin of the dark material on Ganymede and Callisto and thus is a top science goal of the JUICE experiments (GB/GD/GE and CA/CB). Therefore, we selected local deposits of high concentrations of dark non-ice material on Ganymede, which is associated to impact craters that could be identified in Galileo and/or Voyager images as potential RoIs (Fig. 12 and Tab. 3). Although the identification of similar features on Callisto is difficult due to the very low visible albedo of the satellite's surface and the poor spatial resolution of the imaging data, a few areas with peculiar dark crater deposits also show up in the SSI images of Callisto (Tab. 4, Fig. 12g). Since, similar to the paterae (category 2), the selected impact craters are rare and, particularly on Ganymede, often relatively small, the highest spatially resolved and coordinated observations of the different JUICE instruments are essential to observe the proposed RoIs. Therefore, priority 3 has been assigned to the RoIs of this category.

As in case of paterae (category 2), impact craters associated with dark deposits are small enough to be observed by a single JANUS and MAJIS observation. Therefore, during the flybys at

Ganymede and Callisto as well as during GCO5000, the geologic and compositional context, i.e. the chemical and physical characteristics of the terrain in which in the impact crater has been emplaced, and the time of the emplacement can be identified. The geologic context is essential to distinguish between excavated subsurface material and residuals of an impactor. In addition, crater morphology and the distribution of the dark deposits with respect to the crater can be studied to characterize the impact event (impact velocity, impact angle) and the trajectory of the ejecta. JANUS color together with MAJIS data can provide first indication of the dark material composition and physical properties and if mineralogically more than one type of dark material (carbonaceous, silicates etc.) exists on Ganymede.

The surface composition and texture of the dark ejecta deposits derived by JANUS, MAJIS and UVS can be verified during GCO500 (Fig. 13). Particularly, MAJIS' abilities (spatial and spectral resolution, SNR) should be able to constrain the dark material properties in the wavelength region between 3 and 5 µm, where absorptions of organic compounds concentrate (Clark et al., 2009). GALA and RIME will provide valuable information about the impact crater formation associated with dark deposits and possible inhomogeneities in the subsurface properties as evidence for or against a possible origin of dark crater material from subsurface units composed of non-icy material. In case of targets with diameter less than 10 km such as dark halo crater Khensu (ID #3.7), from the 276 possible JANUS images at least 33 are needed in GCO500 to map the entire impact feature, its dark halo and ejecta in detail (Fig. 13 a and b). Partially off-nadir pointing could be necessary for JANUS and MAJIS to entirely cover the feature. Nevertheless, small features such as dark ray craters often exhibit far extending ejecta deposits, which are particularly interesting because of their high concentration of dark non-ice material. In case of impact crater Kittu (ID #3.1) about 1015 JANUS images are needed to cover the impact feature completely (Fig. 13 c). In

case of data volume or observation time constraints it could be necessary to either a) select observations, which enable to derive a profile showing the transition from crater interior to outer portions of the ejecta blanket (Fig. 13 d; 191 JANUS images), b) observe only a subset of the area covering the crater and the nearest portion of the ejecta (Fig. 13 e; 176 JANUS images), or c) the observations could be limited to local spots (Fig. 13 f; 48 JANUS images) depending on the scientific focus of the specific JUICE instrument. In case of the imaging and spectral imaging instruments this could be the crater itself and several spots in the ejecta blanket. In any case, the development of the ejecta composition with growing distance from the crater can be investigated and changes in ejecta properties/composition (colour) due to changes in the substrate or gradient in the ejecta composition with growing distance from the crater should be possible to be studied.

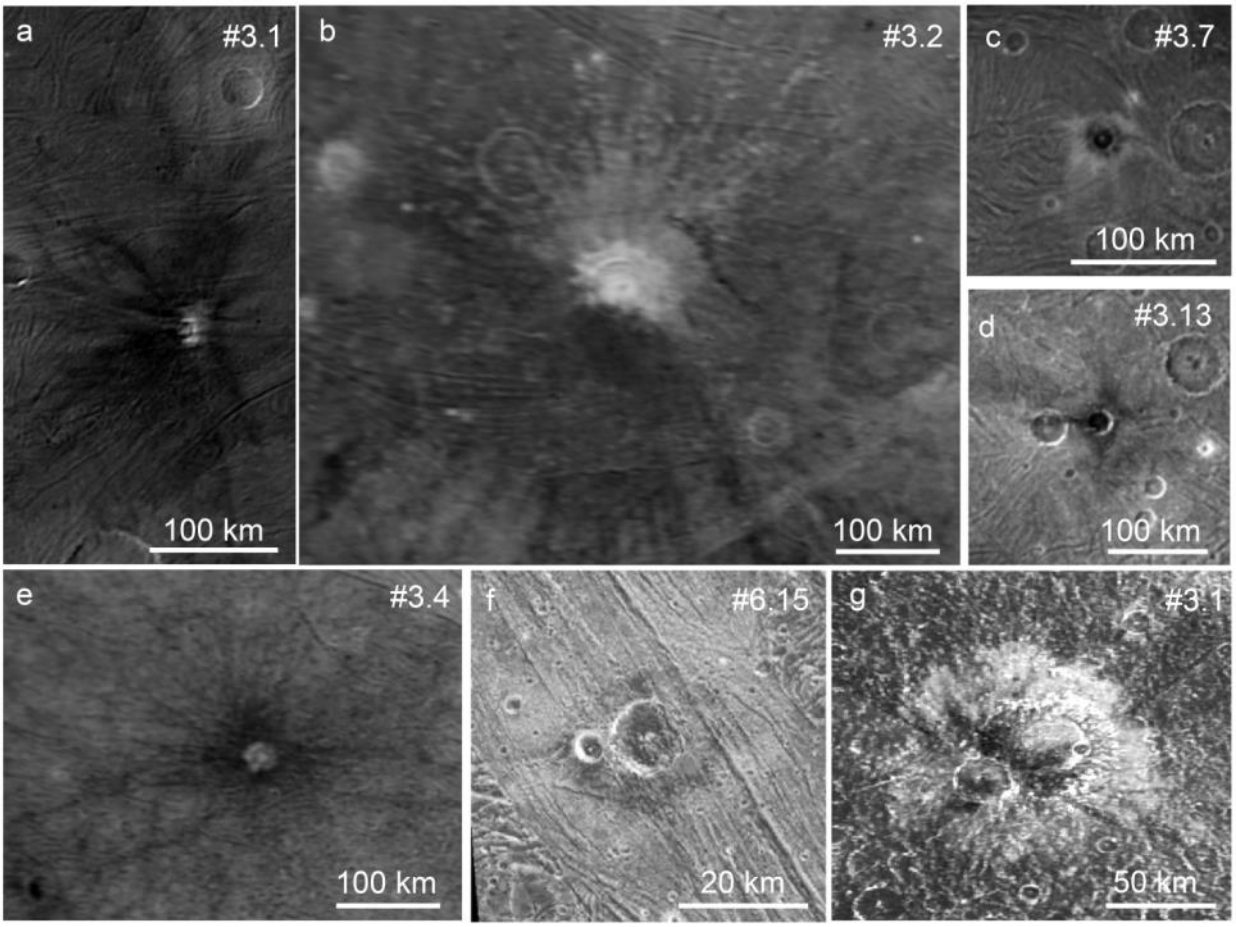

Figure 12: Examples of dark ray, floor and halo craters on Ganymede (a - f) and Callisto (g) proposed to be observed during the JUICE mission. Some of very small dark impact craters are incorporated in RoIs of other categories such as f) the small impact crater Nergal (38.6°N/159.5°E) in Byblos Sulcus (ID #6.1.5).

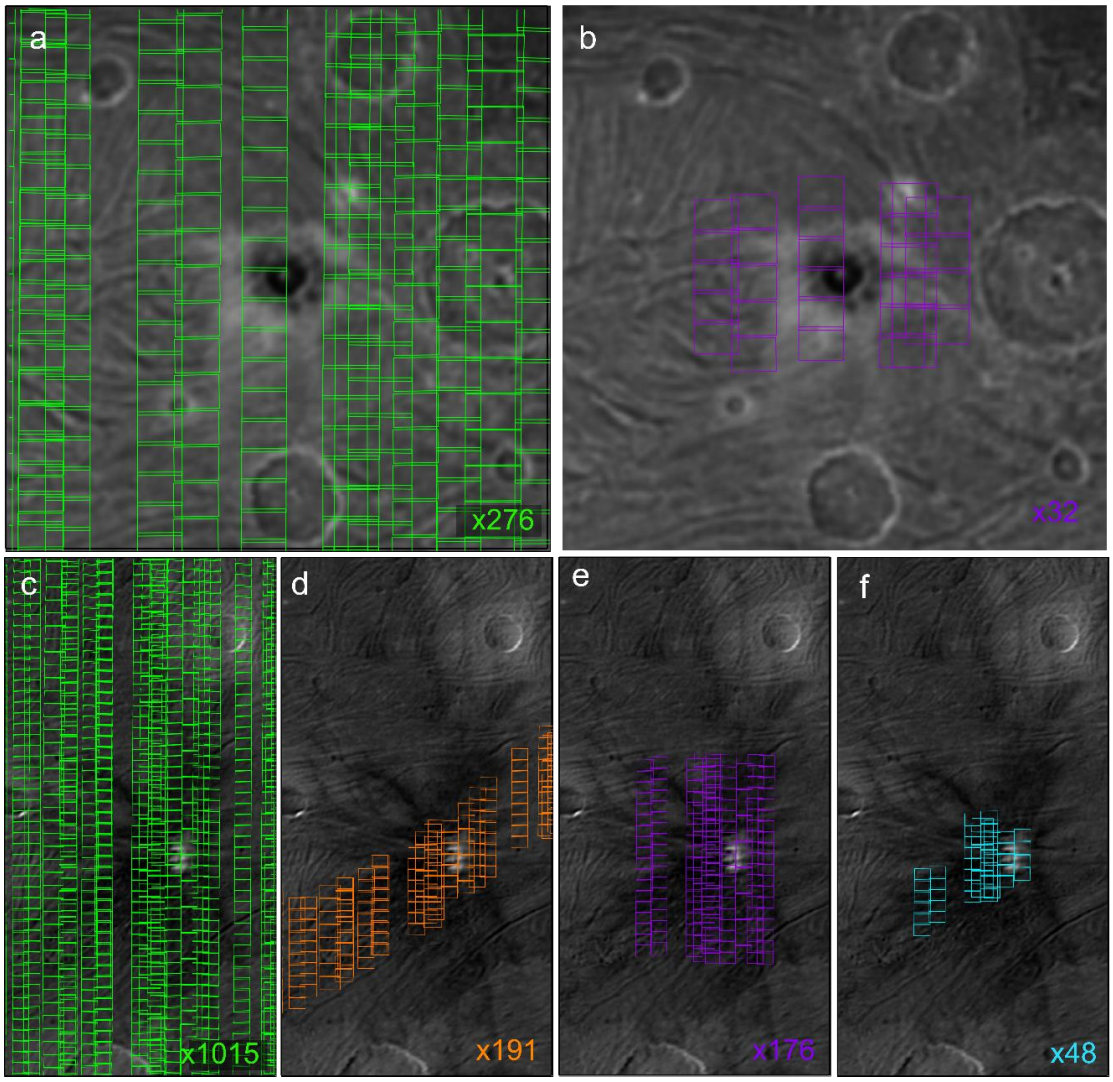

Figure 13: JANUS GCO500 coverages of RoIs #3.7 and #3.1: a) 276 available GCO500 observations and b) the minimum number of 32 GCO500 observations required to investigate impact crater Khensu (ID # 3.7, crater diameter: 17 km) in detail and c) 1015 available GCO500 observations to study impact crater Kittu (ID #3.1, crater diameter: 15 km) with d) 191 JANUS image to study variations across the impact crater and its ejecta blanket (orange), e) 176 images covering the impact crater itself and the ejecta deposits closest to the crater (violet) and f) at least 48 images necessary to cover the crater and a small spots of the ejecta blanket (cyan).

4.4 Impact Crater Morphologies and Catenae

Ganymede and Callisto exhibit the greatest variety of impact crater morphologies among the icy satellites with several of them being unique in the Solar System. The different morphologies are considered to be due to the mechanical properties of ice or the presence of liquids in the subsurface and thus mirror the properties of the target's icy subsurface at the time of the impact event (Bray et al., 2012; Luttrell and Sandwell, 2006; Schenk, 2002) and long-term relaxation of the impact topography (Dombard and McKinnon, 2006). Studying these impact crater morphologies applies to several JUICE science objectives. It not only furthers our understanding about impact cratering processes on icy bodies, but also the characterisation of the satellite's ice shell (GB, CA) including implications for the thermal state at the time of the formation of the feature, the stratigraphy and evolution of the subsurface properties including changes in the heat flow (CC, GD) and the accessibility, interaction and habitability of subsurface oceans (GA).

The selected RoIs present impact craters of all so far identified impact crater morphologies (Fig. 14) and divided into subcategories based on their major morphological characteristics. The morphologies range from relatively fresh simple bowl-shaped craters to complex craters with (0) central peaks, (I) central pits, (II) central domes, but also (III) topographically elevated ejecta blankets (pedestals) (IV) palimpsests or penepalimpsests and (V) large multi-ring impact basins (Schenk et al., 2004). It has to be noted that the number of subcategories does not necessarily imply a process in the transition from one impact morphology to another. We did not define a subcategory or specific RoIs for fresh impact craters with a bowl-shape, i.e. simple craters (Fig. 14 a), though. These craters are usually very small (< 3 km) (Schenk et al., 2004), widely distributed and therefore presumably often appearing within other RoIs. In addition, some impact craters show the

characteristics of at least two different morphologies such as impact craters showing a central pit with a smaller peak in its center (Fig. 14 d) or pedestal craters with and without central peaks (Fig. 14 i - l). Such craters possibly represent key features in the investigation of how a specific crater morphology changes into the other. Selected complex craters have been chosen also depending on their geologic context, i.e. the terrain type they have been emplaced in. Few impact craters, such as Melkart (Fig. 15), lie directly at the border between two terrain types and offer a detailed look for differences in the morphology and composition of the crater material with varying substrate. Others lie within the region of giant impact basins, such as dome crater Doh on Callisto (ID #4.3.3) within the impact basin Asgard. Complex craters with an extended system of ejecta rays have been included into target category 5. Since these craters are very young, they are a highly valuable stratigraphic marker with information about the recent target properties and can be combined with all other results to describe the evolution of the crustal properties with time.

Furthermore, sometimes several hundred kilometres-long impact crater chains (*catenae*) on Ganymede and Callisto have also been included in this category, although they are strictly speaking not a different type of crater morphology. Catenae are thought to have been formed by the impact of a body that was broken up by tidal forces into a sequence of smaller objects such as comets following roughly the same orbit (Schenk et al., 1996). Their investigation enables a better definition of the dynamical and physical properties as well as mass/size distribution of the impactors in the Jovian system. Impact craters of varying morphologies are ubiquitous on both satellites. Nevertheless, attention has to be paid to observe a sufficient number of specimens of varying size and changing substrate and location for each subcategory to be able to investigate the conditions of transformations from one morphology to the other. Therefore, priority 4 has been assigned to this category.

A global coverage of Ganymede in GCO5000 with panchromatic JANUS images would enable mapping the distribution of catenae across the surface to strengthen our understanding of their origin and to study possible implications for Ganymede's orbital evolution including a period of non-synchronous rotation of Ganymede's outer ice shell (Schenk et al., 2004; Zahnle et al., 2003), and to distinguish catenae from secondary impacts of Ganymede's large impact craters (Schenk et al., 2004). JANUS images acquired during GCO5000 will enable to characterize the substrate, the type of crater morphology, transition parameters from one to the other type in detail and to put the individual craters into a chronological context. JANUS colour images, MAJIS and UVS data acquired during GCO5000 provide first insight into the relationship between impact crater morphology and physical and chemical surface properties including subsurface, when sampling the excavated materials (see below).

These data will be complemented in GCO500 by GALA/JANUS topography revealing details of the inner-crater structures such as peaks, pit, domes and ejecta of pedestal craters, which are essential to study the formation process and conditions necessary to build the corresponding morphology. Topographic data are also essential to distinguish between morphological characteristics established during and/or subsequently after the impact event (Luttrell and Sandwell, 2006) and viscous crater relaxation over time (Bland et al., 2011).

Highest resolution MAJIS and UVS data from GCO500 could reveal minor amounts of impurities in the surface ice such as volatiles and salts and organics, which could be essential to fully explain the formation process. Together with SWI and RIME data, interactions with possible liquids in the subsurface and Ganymede's or Callisto's subsurface ocean could be revealed. In particular, RIME can detect the base of pedestal craters through structure and impurity profiles, thus help in inferring the composition of the elevated ejecta blanket (Thakur and Bruzzone, 2021).

Since many of these impact craters are relatively large (diameter > 100 km) with partly extended ejecta deposits, care has only to be taken which portions of the specific impact crater are essential to be observed at the highest possible spatial resolution in case of data volume constraints. Given a full coverage during GCO5000, losing spatial resolution of the imaging and spectral imaging due to binning, should be the last choice. When investigating impact crater morphologies, the details, such as the central peak, pit, or dome, as well as the elevated ejecta blanket of pedestal craters, are the most important, because they define the specific morphology. Therefore, similarly as for the impact craters in category 3 (Fig. 12), one must either only observe the crater, perform a profile across the centre of the impact crater including the ejecta deposits, or only image the most important spots (peak, pit or dome etc.). However, observing individual spots might be sufficient for local morphology, topography, surface age measurements and local concentration of impurities. High resolution MAJIS observations of relatively young impact craters, in particular dome craters such as Melkart (Fig. 14), could provide unprecedented views into the possible content of volatiles in the uplifted and excavated crustal material exposed in the central dome.

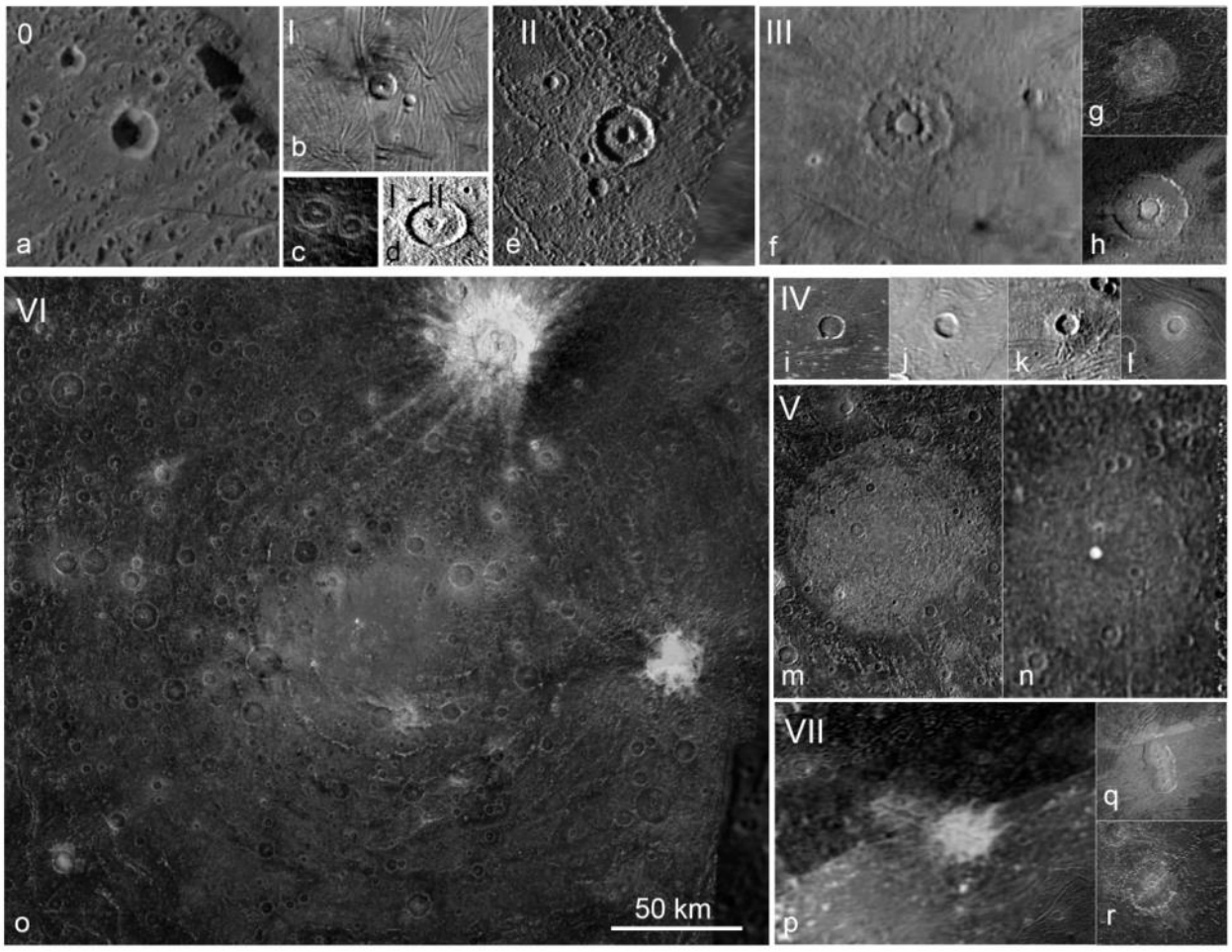

Figure 14: Examples of impact crater morphologies (category 0 - VI) on Ganymede (G) and Callisto (C): a) simple bowl shape (0), b) and c) central peak (I), d) and e) central pit (II) partly showing the transition from peak to pit (I – II), f) – h) central dome (III), i – l) pedestal (IV) and m) – n) palimpsest (V); o) multiring impact basins; and p – r) catenae (VII) with the RoI IDs b) (G) #4.1.1, c) (C) #4.1.1., d) (G) #4.2.4, e) (G) #4.2.1, f) (G) #4.3.6, g) (C) #4.3.2, h) (G) #4.3.2, i) (G) #4.4.5, j) (G) #4.4.3, k) (G) #4.4.11, l) (G) #4.4.6, m) (G) #4.5.2 n) (C) #4.5.1 o) (C) #4.6.1 (scale bar fits to all images), p) (G) #4.7.3, q) (G) #4.7.4, and r) (C) #4.7.1.

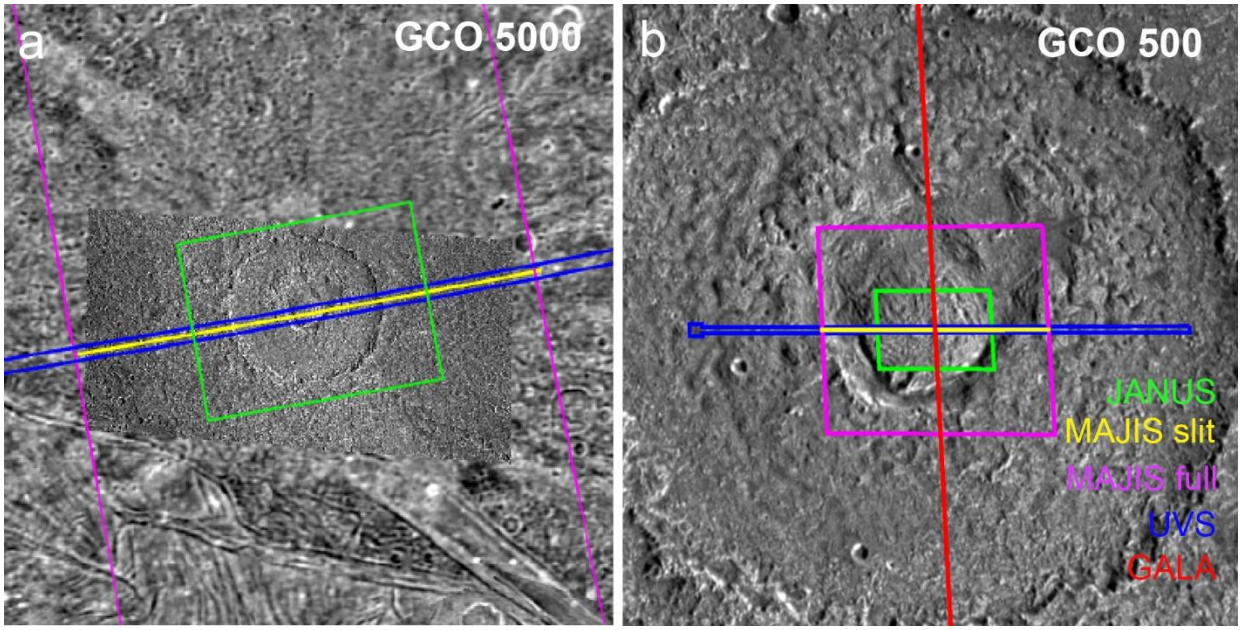

Figure 15: Footprints of different JUICE instruments (JANUS (green), MAJIS FOV built over time (magenta), MAJIS single slit pointed at boresight (yellow), UVS (blue), GALA (red) during the a) GCO5000 and b) GCO500 for impact crater Melkart (RoI #4.3.1, 105 km) with its extended ejecta deposits. Please note that GALA will not operate during GCO5000.

4.5 Bright Ray Craters

Bright ray craters are the most abundant type of impact craters on Ganymede's and Callisto's surfaces. They represent some of the youngest surface features on both satellites, and are thus an important stratigraphic marker for the youngest geologic period on both satellites (Wagner et al., 2019a). Furthermore, their ejecta deposits represent relatively un-weathered material excavated from the subsurface and therefore offer the possibilities to directly study the composition of Ganymede's and Callisto's uppermost ice crust, which is an essential element of the JUICE science

objectives (GA/GB/GD/GE/CA; Fig. 6). Depending on their size, each of these impact craters probe a different depth of Ganymede's and Callisto's crust and could enable to develop a stratigraphic profile of the crustal composition. Of particular interest are the physical properties of H_2O ice, and any contents of impurities such as volatiles like CO_2 incorporated in the subsurface ice as already implied on Callisto (Hibbitts et al., 2002), and salts (Ligier et al., 2019) and any variations of the subsurface composition depending on different terrain types.

To probe bright ray craters of the largest possible range of excavation depths, we propose a set of fresh bright ray craters with crater dimensions from a few to up to almost 200 km as potential RoIs (Fig 14). All RoIs are located between +/- 60° latitudes to avoid the influence of polar deposits, which could easily mask the original properties of the excavated subsurface material (Figs. 5 and 6). Since bright ray craters are ubiquitous on Ganymede's and Callisto's surfaces, priority 5 has been assigned to this category. However, attention has to be paid to observe bright ray craters covering a wide range of sizes and locations in different terrain types. In addition, because these impact craters also display different morphological characteristics, which have not been modified through time, they could be used as additional RoIs for category 4.

During the flybys at Ganymede and Callisto as well as in GCO5000, the geologic and compositional context of the selected craters, the major characteristics of the individual impact crater and its associated deposits can be identified and mapped by the JUICE imaging and spectral imaging instruments (Fig. 6). JANUS clear-filter images provide first indications of their geologic age, while JANUS colour data combined with UVS and MAJIS spectroscopic data could indicate possible variations in the crustal composition across the icy surface depending on the terrain type in which the impact craters were emplaced. Due to the dominance of the spectral signature of H_2O ice, however, the best possible SNR is needed to identify and map the usually weak and/or narrow

absorptions of volatiles, salts and any other minor compounds. The investigation could be done in comparison with bright ray craters located at higher latitudes such as Osiris (category 1; Fig. 15), which can reveal important information about how polar deposits affects composition, morphology and texture of the crater materials and can therefore be distinguished from fresh crater material (Stephan et al., 2020).

Highest-resolution imaging during GCO500 will enable the usage of fresh impact craters as stratigraphic markers, i.e., to include measurements of the size-frequency distribution of superimposed smaller impact craters to derive relative ages and to strengthen stratigraphic findings from superposition criteria already seen in GCO5000 data. In addition, highest-resolution data can help to distinguish smaller primary from secondary craters (Wagner et al., 2019b). During GCO500 the combination of composition and morphology with topography obtained by GALA of the crater rays can help verifying the time needed until the bright rays are completely faded depending on the content of possible impurities of the crater material and the local environmental conditions (UVS/MAJIS/SWI). Local geologic compositional information will reveal any trace compounds and other local spectral variations in the crater properties, how ejecta deposits affect the surface properties, and particularly large impact events affect the subsurface properties (RIME/3GM) (Fig. 6). Because relatively large examples of bright craters require a high volume of GCO500 observations strategies such as those discussed for RoIs of categories 3 and 4 have to be applied in case of time and/or data volume constraints.

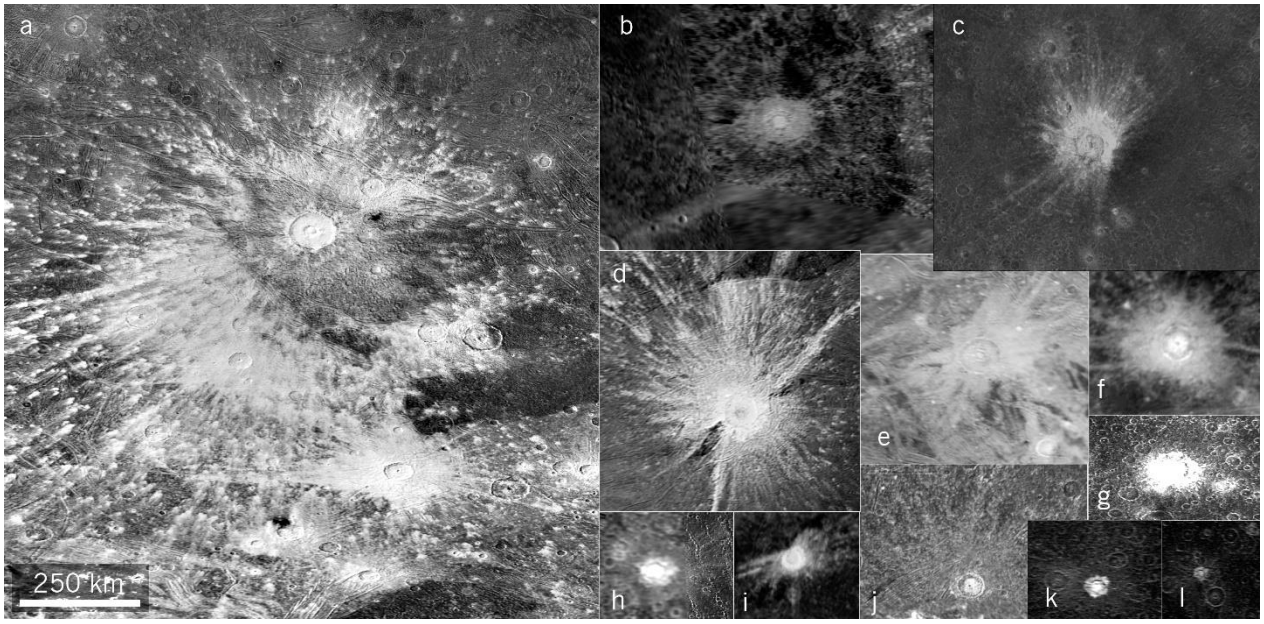

Figure 16: Examples of bright ray craters of different sizes on Ganymede (G) and Callisto (C): a) Osiris (G) #1.03, b) Punt (G) #5.03, c) Burr (C) #5.04. d) Tros (G) #5.02 e) Amon (G) #5.01, f) Ishkur (G) #5.7, g) Agloolik (C) #5.06, h) Nirkes (C) #5.02, i) Apophis (G) #5.05, j) Laomedon (G) #5.11, k) Vili and l) unnamed (C) #5.14 and #5.21, respectively. Selected impact craters on Ganymede can be located in dark and bright terrain. Note that because of Osiris' location at mid-latitudes with influence of Ganymede's polar caps, the crater is primarily a target of category 2. The scale for Osiris fits to all images. The location of the individual RoIs can be seen in the map of Figures 7 and 8.

4.6 Bright terrain

A significant portion of Ganymede (~ 64 %, Patterson et al., 2010) is covered by the so-called bright terrain (Pappalardo et al., 2004 and references therein). Several theories explaining the

formation of Ganymede's bright terrain and its non-occurrence on Callisto are currently under discussion. Although numerous detailed studies of tectonic resurfacing on Ganymede based on Voyager and Galileo data (Bland and Showman, 2007; Bland et al., 2010; Bland and Wyrick, 2017; Cameron et al., 2019; Collins, 2006; Collins et al., 1998; Pappalardo and Collins, 2005; Rossi et al., 2018) support an extensional tectonic model of the bright terrain formation, several aspects, which are related to the JUICE science objectives (GA/GB/GD/GE/CA/CC; Fig. 6), are still unanswered including: Which internal processes (differentiation, phase changes, and/or internal convection of mantle material) or conditions in its orbital evolution (decrease of tidal and rotational distortion, increased spin rate, orbital resonances, non-synchronous rotation) caused the formation of the bright terrain on Ganymede and not on Callisto? hen in Ganymede's evolution did the formation occur and how long did it last (Pappalardo et al., 2004). How did the tectonic styles change during the period of bright terrain formation? What was the role of volcanism at the beginning of the bright terrain formation? Do geologically active regions still exist? Does the bright terrain formation enable to transport material from Ganymede's subsurface ocean to the surface? Are any materials other than H_2O ice involved in the formation process?

Surface features associated with the bright terrain formation range from individual troughs or furrows to complex networks of cells of bright terrain (Pappalardo et al., 2004; Schenk et al., 2001). Individual cracks inferred to define furrows crossing Ganymede's ancient terrain might present the precursor unit of a tectonic resurfacing process (Patterson et al., 2010) and perhaps reactivated older zone of crustal weakening. Possibly, the rare linear features on Callisto, which are related or unrelated to impact events also represent sign of initial tectonic resurfacing. Individual bands of bright terrain dominated by subparallel grooves and ridges show a more progressive resurfacing, which displays its strongest development in extensive areas of a complex network of lanes and

polygons (Patterson et al., 2010). Each of the lanes and polygons represent a set of roughly evenly spaced grooves and ridges oriented in a single dominant direction with the density and the orientation of the structural grooves differing between the individual "cells". Of particular interest are morphologically very smooth polygons with groove structures that are faint or undetectable at the 10s or 100s of meters spatial resolution of the best resolved Galileo images. Cryovolcanic resurfacing may have played a more dominant role in the formation of this smooth terrain (Patterson et al., 2010) and might be related to the formation of the paterae discussed in section 4.2. Furthermore, the rare and unique style of structural modification of the so-called reticulate terrain on Ganymede (Collins et al., 2013; Murchie and Head III, 1986; Patterson et al., 2010), which are dominated by two sets of nearly-orthogonal grooves resembling horst and graben structures, might also represent relicts of the resurfacing of ancient terrain.

Despite the high complexity of the bright terrain, numerous opportunities will exist to observe the RoIs selected for the bright terrain. Furthermore, since bright terrain works as a substrate for many local features included in the RoIs of the categories discussed before, a lot of already defined/selected RoIs enable the investigation of the bright terrain (Tab. 3). Therefore, priority 6 has been assigned to the RoIs of this category. Nevertheless, each of the individual tectonic styles introduced above holds unique geologic and compositional clues about the formation process of the bright terrain, i.e. how the ancient terrain was torn apart or resurfaced to form the bright terrain, and the overall evolution of the bright terrain (Collins et al., 1998). We subdivided the proposed RoIs into the following subcategories (Fig. 17 and Tab. 3 and 4) to enable a thoroughly investigation of Ganymede's bright terrain by the different JUICE instruments:

6.1 - cracks/furrows

6.2 - individual bands

6.3 - complex network of lanes and polygons of bright terrain.

Subcategory 1 includes portions of Ganymede's dark ancient terrain crosscut by the oldest systems of furrows on Ganymede (Fig. 17 a, b). Few RoIs have been also defined for Callisto in this subcategory 1, which cover linear surface features (Fig. 17 c, Tab. 4) that resemble the furrows in Ganymede's dark terrain (Moore et al., 2004; Schenk, 1995) and could help to distinguish between linear features formed related or unrelated to impact events. Subcategory 2 contains individual bands of bright terrain resembling grooved or smooth portions of the bright terrain (Fig. 17 d, e) as described in Patterson et al. (2010). In contrast, RoIs of subcategory 3 cover regions, in which cells of both grooved and smooth terrain form a complex pattern. Because, Ganymede's reticulate terrain is always surrounded by extensively resurfaced regions of bright terrain (Patterson et al., 2010), the corresponding RoIs are also included in subcategory 3 (Fig. 17 h). Few RoIs have been defined for subcategory 3, which appear to have similar morphological characteristics like surface features that previously have been only observed on Europa (and the Saturnian satellite Enceladus) such as chaotic terrain and double ridges (Fig. 17 i, j). Detecting relicts of such features on Ganymede could provide evidence that European-like resurfacing processes took place in Ganymede's past. Furthermore, the RoIs of these categories also include key areas for studying the a) transition/contact between the ancient and the younger bright terrain (Fig. 17 b, c), b) en echelon structures, fault duplexes, lateral offsets (Fig. 17 d) and tectonically-influenced surface features such as impact craters (Fig. 17 f) to study the kinematics and structural evolution of grooves and to quantify the deformation of these features (Pappalardo and Collins, 2005).

During the flybys at Ganymede as well as during GCO5000 the different tectonic styles seen in the bright terrain can be identified and morphologically characterized based on JANUS images including the investigation of their stratigraphic relationships, the measurements of their geologic age and the duration of the bright terrain formation. Furthermore, the GCO5000 JANUS images together with GALA topography will allow the measurement of the total amount of strain and strain rates implied by the global distribution of bright terrain (Pappalardo and Collins, 2005; Pappalardo et al., 2004; Collins et al., 1998). Those measurements are still confounded by the uneven nature of the currently available data coverage impeding uniform morphological classification and available topographic data set of the satellite (Collins et al., 2009), but are essential for a deeper understanding of the processes causing the complex formation of the bright terrain. Furthermore, JANUS colour data can indicate regional compositional variations within the bright terrain, which will be complemented by variations in the surface composition provided by MAJIS and UVS. Of special interest is the occurrence of impurities such as salts as predicted by telescopic observations (Ligier et al., 2019), which could be a potential driver of the formation process.

During GCO500, imaging data accompanied by topographic information from JANUS stereo imaging and GALA will enable to characterize the contact between ancient and bright terrain and quantify the conditions of the local tectonic movements. Surface compounds detected and mapped by MAJIS and UVS in GCO5000 can be verified and associated with specific local geologic and geomorphologic surface features within the bright terrain. In addition, subsurface properties provided by RIME, SWI and 3GM could reveal the nature of tectonic deformation (Heggy et al., 2017; Sbalchiero et al., 2019), and any connection of the bright terrain formation with subsurface structures and ocean including any signs of the ocean's chemistry and biology. Particularly, RIME

will be able to detect any buried evidence of resurfacing in the bright terrain, except when the surface is highly smooth and specular (Thakur and Bruzzone, 2021).

The strategy to limit the GCO500 observations should differ with subcategory. The observation of cracks/faults and narrow band observations could be constrained onto the linear feature itself (Fig. 17). They should also cover the local appearances of the reticulate terrain. However, in case of long bands and the extended regions of complex networks of bright terrain with more scientifically important local spots, a more detailed strategy is necessary. Because of the limited spatial resolution of the recently available data, these sub-RoIs should be refined, when the first Ganymede data of the flybys and GCO5000 data with a sufficient spatial resolution become available. However, depending on the science objectives, these sub-RoIs could be selected for observing a profile across the borders of a tectonic feature covering the area of contact to the neighbouring dark terrain as exemplary shown for a portion of the bright terrain of Uruk Sulcus (RoI #6.3.2) (Fig. 18, white frames), which would allow to evaluate the local formation of the bright terrain. Here and in many other areas Ganymede's bright terrain consists of many 'cells' of varying age, tectonic orientation and style (Fig. 18, green frames). Therefore, sub-RoIs should also cover the different tectonic styles, their direct contact to each other and, if applicable, to the neighbouring ancient terrain to gain a deeper understanding of the bright terrain formation. Particular care should be taken to observe the smoothest portions of the bright terrain, as the high spatial resolution achievable during GCO500 is needed to resolve details in their tectonic style and to reveal signs of past cryovolcanic activity. Finally, small and presumably fresh either dark or bright impact craters (Fig. 18, red frames) are valuable stratigraphic markers with respect to age and subsurface composition of the bright terrain and should be also imaged in GCO500.

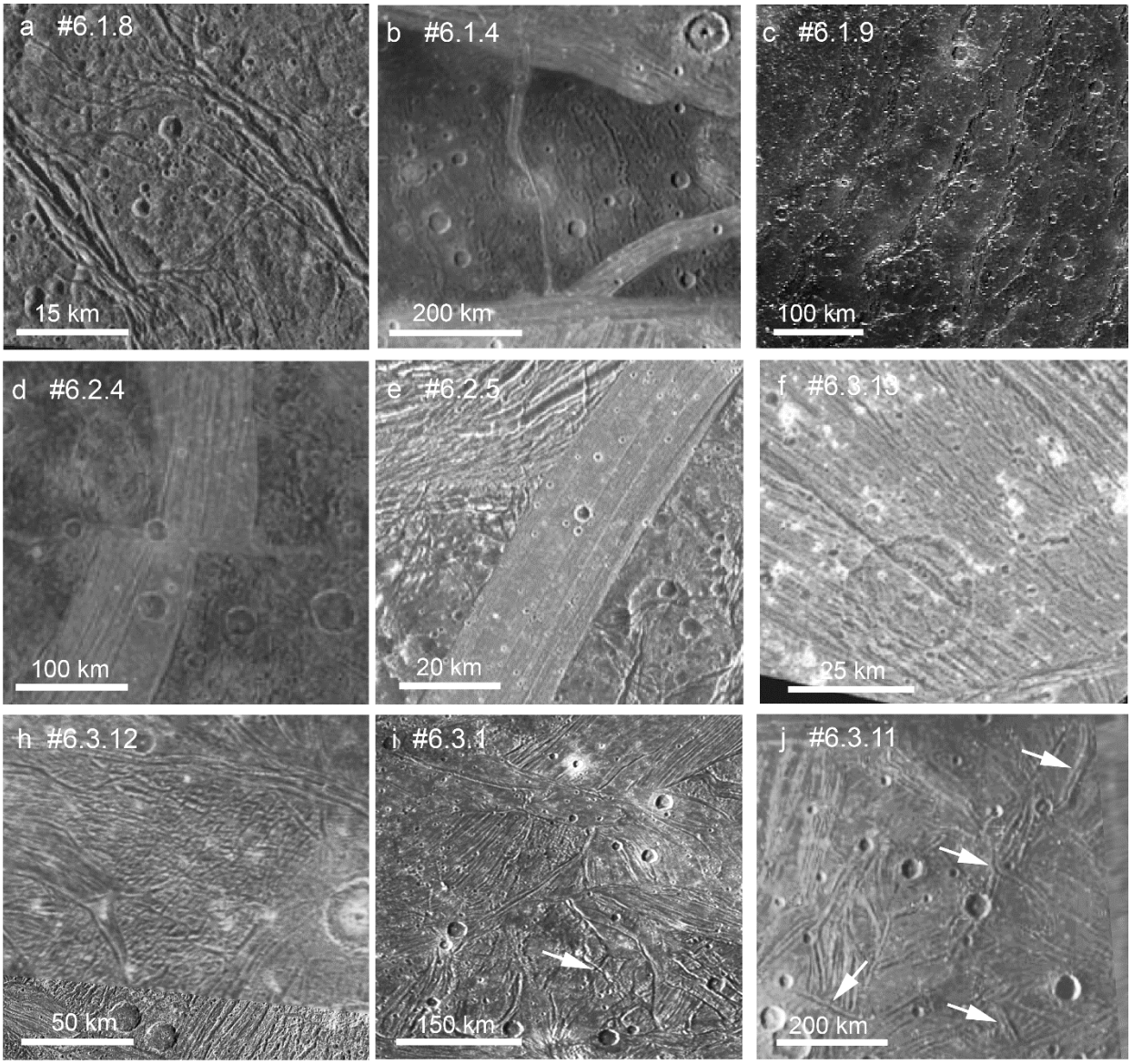

Figure 17: Examples of RoIs for the investigation of Ganymede's bright terrain and furrows on Callisto: 1) category 6.1: a) furrows in Ganymede's ancient dark terrain and b) on Callisto, 2) category 6.2: d) and e) individual bands (partly showing tectonic movements), and 3) category 6.3: complex network of bright terrain including f) distorted impact craters, h) reticulate terrain and j) regions showing possible relicts of Europa style resurfacing (indicated by white arrows) including j) double ridges. IDs of the RoIs are indicated.

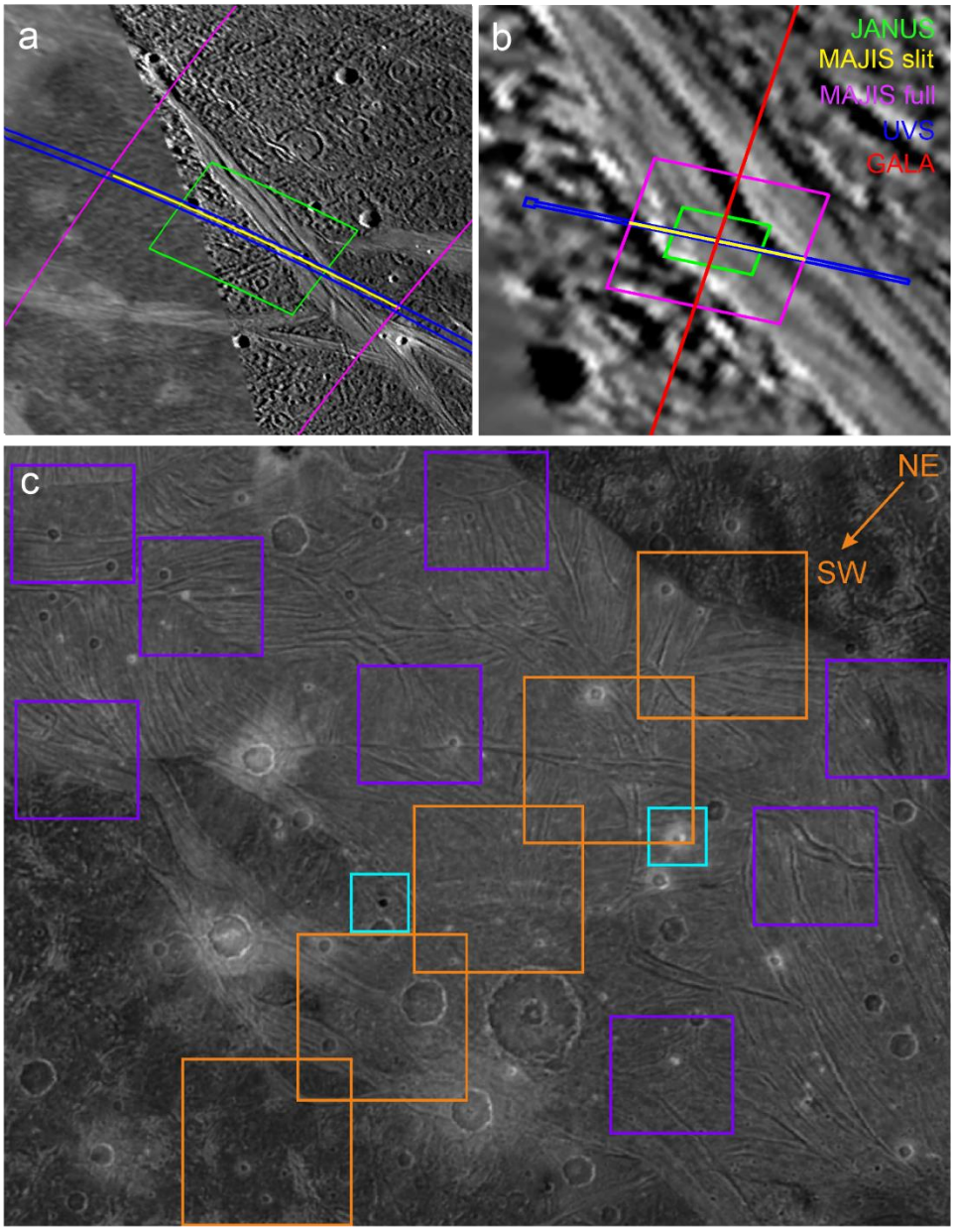

Fig. 18: Footprints of different JUICE instruments (JANUS (green), MAJIS FOV built over time (magenta), MAJIS single slit pointed at boresight (yellow), UVS (blue), GALA (red) during a) GCO5000 (Please note that GALA will not operate during GCO5000.) and b) GCO500 for a tectonic band in Marius *Regio* including a small dark halo impact crater (RoI #6.1.3, ~300km); as well as c) possible sub-RoIs within RoI #6.3.2 (~500 x 500 km) to be observed during GCO500

with the highest level of details in case of data volume and/or time constraints during GCO500: 1) profile across Uruk Sulcus (orange frames), 2) contact regions of different tectonic 'cells' within the bright terrain, which exhibit different structural orientation and/or tectonic style (violet frames), 3) small fresh dark or bright impact craters (cyan frames) revealing fresh subsurface material.

4.7 Dark Terrain

The ancient heavily cratered terrain, which comprises about 1/3 of Ganymede's and most of Callisto's surface, is characterized by a high concentration of the visually dark non-ice material for a thin layer on top the satellites' icy crust (Prockter et al., 2000; Prockter et al., 1998). Although, its spectral properties indicate a composition similar to carbonaceous chondrites (McCord et al., 1997, Hibbitts et al., 2003, Molyneux et al., 2020), its mineralogical composition is far from being resolved (Ligier et al., 2019). The investigation of the detailed chemical and physical properties, particularly its potential content of organic material, its nature and origin are one of the top JUICE science objectives (GE/CB). Furthermore, these ancient terrains are the regions that are mostly affected by weathering processes such as micro-meteoritic bombardment, sublimation and radiation by magnetospheric plasma (Moore et al., 2004) and thus are the best place on both bodies to study the weathering effects onto the surface composition, morphology and topography in combination with the local environmental conditions.

Consequently, we selected a set of RoIs across the equatorial regions ($< \pm 40°$ and away from the polar caps) of both satellites dominated by dark material. On Ganymede, these RoIs are located within Ganymede's ancient dark terrain called '*Regiones*' (Prockter et al., 1998, Pappalardo et al., 2004) (Fig. 18). We defined RoIs in the largest *Regiones*, i.e. Marius, Perrine, Nicholson and Melotte *Regio*. On Callisto, most of the surface is characterized by a thick layer of fine-grained

dark material (Moore et al., 2004). The defined areas include numerous more or less degraded impact features (Fig. 19). Therefore, together with the impact craters selected as RoIs for category 4, these craters could be used to investigate impact crater morphologies in different relaxation states to better understand the history of heat flow in the subsurface of both bodies and to distinguish between effects of exogenic influenced surface degradation from crater relaxation processes with time (Bland et al., 2017). Additional surface features appearing in a specific RoIs are indicated in the description of the corresponding RoI in table 3 and 4.

Nevertheless, because the ancient dark terrain on Ganymede and Callisto and thus the dark non-ice materials are abundant on both satellites, as opposed to dark, non-ice material related to fresh impact craters (target category 3), numerous opportunities will exist during the JUICE mission to observe it. In addition, ancient dark material also occurs in many RoIs of most of the other categories as substrate of selected impact craters (categories 2 to 5, Fig. 19) and neighbouring terrain (category 6.1 and 6.2) (Fig. 19). Thus, priority 7 has been assigned to the investigation of the ancient dark terrain.

During the flybys at Ganymede and Callisto as well as GCO5000, JANUS color images, MAJIS as well as UVS data will characterize the spectral signature of the dark non-ice material with first implications for its mineralogy and content of volatiles such as CO_2 (Hibbitts et al., 2002, 2003). Of particular interest is the comparison between the surface compounds of the dark material on Ganymede and Callisto (Hibbitts et al., 2002, 2003, Molyneux et al., 2020), which could resolve 1) if more than one type of dark material exists on Ganymede (carbon-rich, sulfur-bearing etc.), and 2) the degree of alteration due to mixing with the surface ice (such as hydroxylation and hydration, release of trapped gases from the subsurface ice through impact processes) and radiation effects (implantation) (Ligier et al., 2019; Ligier et al., 2016; Trumbo et al., 2019). JANUS images

in combination with topography information of GALA and thermal surface and subsurface properties derived by SWI and RIME are important to characterize the geologic (including its age) and geophysical context of the individual surface compounds related to the dark material. Of particular interest will be the comparative observation of the styles of surface degradation on both satellites and the resulting mass wasting features (Moore et al., 1999, 2004).

During GCO500, the spatial resolution of the spectral imaging data (UVS and MAJIS) might reveal the signature of organic compounds (McCord et al. 1997, 1998). The spectral signatures of organics are hard to detect, when mixed with H_2O ice, so that high spatial resolution is a key to investigate visually dark, relatively ice-free patches that could provide unequivocal evidence. In addition, imaging and spectral data sets (UVS, JANUS, MAJIS) together with topographic (GALA) and thermal data (SWI) achieved during GCO500 enable to characterize the weathering processes at a local scale and quantify local small-scale surface degradation including mass wasting features as seen in Galileo images of Callisto (Moore et al., 1999; Moore et al., 2004) and the infills of topographic lows by dark non-ice material (Prockter et al., 1998, Pappalardo et al., 2004). These data will be complemented by RIME data, which can also be used to estimate the presence of dust-rich impurities in the ice on Ganymede and Callisto, and particularly the thickness of the dark terrain regolith (Heggy et al., 2017; Sbalchiero et al., 2019). Finally, PEP and RPWI can provide the exogenic environment of the equatorial regions of both satellites, which could significantly differ from the polar region (especially for Ganymede).

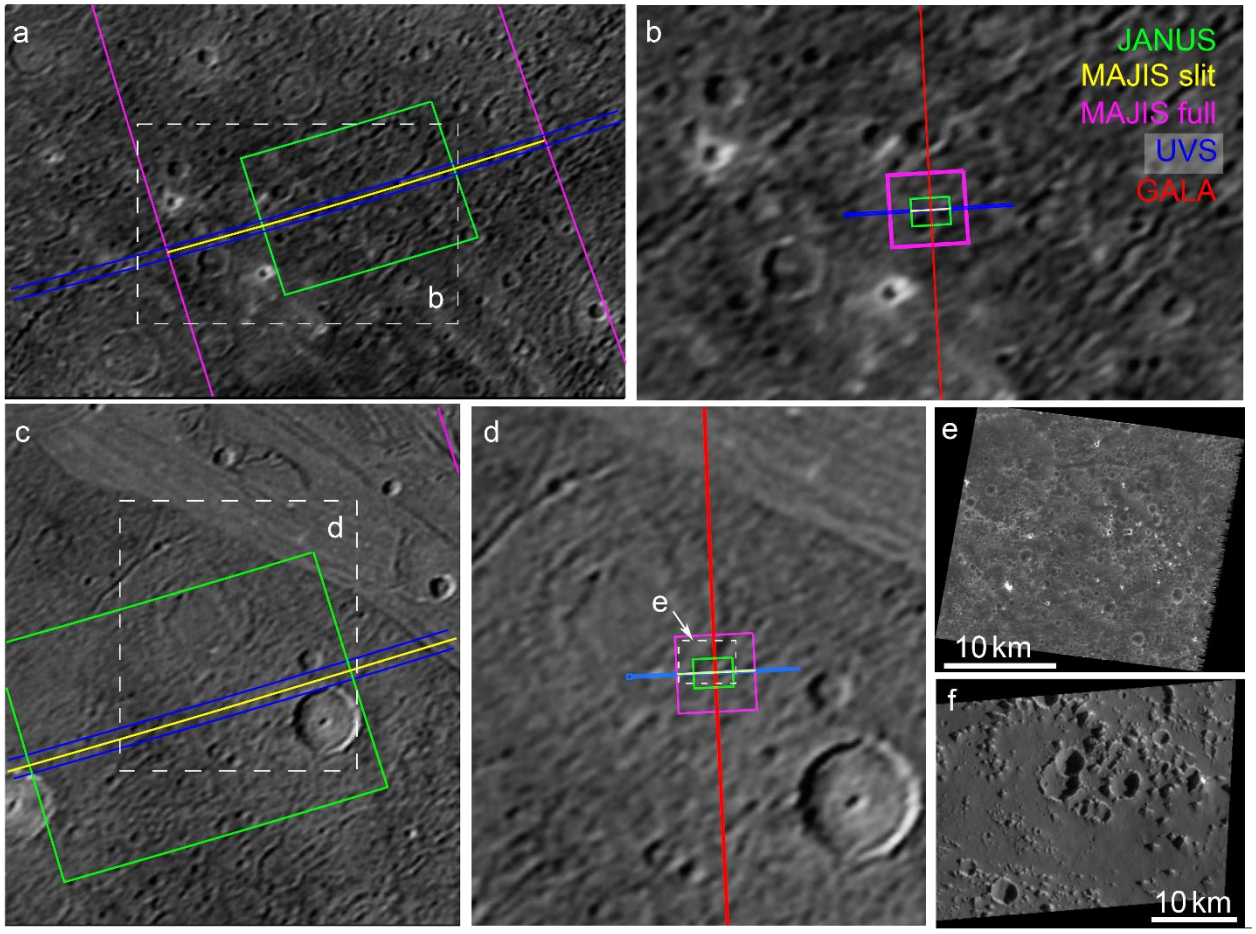

Figure 19: Examples of selected target regions for the investigation of the ancient dark terrain: 1) portion of Nicholson Regio selected for RoI #7.5 overlaid by single footprints possible during a) GCO5000 and b) GCO500 and 2) portions of Nicholson Regio surrounding an ancient palimpsest selected as RoI#4.5.14 (as an example of dark terrain seen in RoIs of other categories) overlaid by possible footprints during c) GCO5000 and d) GCO500, which include e) the portion of Nicholson Regio on Ganymede observed by Galileo SSI (~10.6°S/34.6°E; ~25 m/pixel) in comparison with f) the dark terrain on Callisto (~22°N/~218°E: ~900 m/pixel) located in the southern portion of the ancient impact basin Asgard, which is covered by RoI #7.1. Please note that GALA will not operate during GCO5000.

5 Conclusions

The proposed lists of RoIs on Ganymede and Callisto's surface have been drawn up to support the observation planning by the JUICE SWT and WGs as well as by the individual instrument teams. It should work as a tool for each instrument team to define baseline observation requirements such as time and data volume constraints, as well as measurement parameters to optimize the synergy of the JUICE instruments. Therefore, the JUICE Operational SPICE Kernel Dataset provided by the ESA SPICE Service (https://doi.org/10.5270/esa-ybmj68p) now accounts for the location and extent of those RoIs, thus allowing to identify opportunities for observation in the planning tools set up by ESA and by the individual JUICE instrument teams. However, only regions that were already observed during the Galileo and Voyager missions with at least intermediate spatial resolution could be included in the present target lists so far. Large regions exist on both satellites, where no RoIs could be defined, making our selection a good starting point that JUICE should be able to expand in the future once new data of the icy Galilean satellites will be acquired. The lists should be continuously updated depending on results and new open science questions, which come up during ongoing and future scientific work (observations by the instruments of the Juno spacecraft, telescopic observations or experimental studies) up to the arrival of JUICE in the Jovian system, and a deeper study of the observation opportunities that will be done after the trajectory is more consolidated (sometime after the launch).

In addition, we may expect that during the flybys, due to the quite long Jupiter orbital phase, we may identify several other regions of interest due to the much higher resolution we will get on most of the satellites' surfaces than before; these regions could then be considered for observations during the following flybys or the Ganymede orbital phases. Finally, the global coverage of

Ganymede obtained during GCO5000 will add further opportunities for the identification of regions of interest, although the proximity in time with the following GCO500 phase will need quite an effort to plan for their observation at the possible highest resolution.

Therefore, an evaluation of the recent Ganymede RoI list could be necessary at least after the first Ganymede flybys have taken place and the first new data of Ganymede are available. Regions that will become visible for the first time with sufficient spatial resolution, could reveal new aspects that are not covered by these RoI lists. Either additional RoIs will be selected or the strategies to observe the already proposed RoIs could change. The same could apply in case of regional concentrations of so far undetected and/or unmapped trace compounds and salty materials not covered by already proposed RoIs and/or the detection of active plumes from the remote distances. In addition, as already discussed, during and after achieving a global coverage by imaging and spectral imaging data, RoIs can be better constrained to smaller areas, i.e. sub-RoIs, to decrease the required observation time and data volume. Finally, note that, at the moment, the current mission profile does not allow significant multitemporal observations by the imaging and spectral imaging instruments. If possible, it should be considered to observe particularly equatorial areas at different times of a day (dawn, sunset) on Ganymede and Callisto to look for signs of spectral variations due to changing competition between space weathering processes (sublimation, plasma bombardment).

6 Acknowledgments

The authors want to thank Geoffrey Collins and an anonymous reviewer for significantly improving this manuscript with their careful reviews. The authors also gratefully acknowledge very helpful discussions with all JUICE working groups and the continuous support by the JUICE

Science Operation Center (SOC) at ESAC. Italian co-authors acknowledge support under the ASI-INAF agreement 2018-25-HH.0. The French co-authors acknowledge the support from CNES. The mission trajectory used for this work is based on JUICE SPICE Kernel Dataset CREMA 3.0. (ESA SPICE Service, JUICE Operational SPICE Kernel Dataset). The global imaging maps produced and provided by USGS (available at https://astrogeology.usgs.gov) from Voyager and Galileo ISS and SSI images were used a baseline for this work.

7 References

Barabash, S., Brandt, P., Wurz, P., and Mission, P. T. J. r. I. W. o. I. f. P., Particle Environment Package (PEP) for the ESA JUICE MissionOctober 01, 2016 2016, Volume 1980, p. 4079.

Bergman, J. E. S., Wahlund, J.-E., Witasse, O., and Cripps, V., 2017, The Radio & Plasma Wave Investigation (RPWI) for JUICE - From Jupiter's Magnetosphere, through the Ice Shell, and into the Ocean of Ganymede, European Planetary Science Congress, p. EPSC2017-2373.

Bland, M., and Showman, A., 2007, The formation of Ganymede's grooved terrain: Numerical modeling of extensional necking instabilities: Icarus, v. 189, no. 2, p. 439-456.

Bland, M. T., McKinnon, W. B., and Showman, A. P., 2010, The effects of strain localization on the formation of Ganymede's grooved terrain: Icarus, v. 210, no. 1, p. 396-410.

Bland, M. T., Singer, K. N., McKinnon, W. B., and Schenk, P. M., 2011, Constraints on Ganymede's Thermal Evolution from Models of Crater Relaxation, Lunar and Planetary Institute Science Conference Abstracts, Volume 42, p. 1814.

Bland, M. T., Singer, K. N., McKinnon, W. B., and Schenk, P. M., 2017, Viscous relaxation of Ganymede's impact craters: Constraints on heat flux: Icarus, v. 296, p. 275.

Bland, M. T., and Wyrick, D. Y., 2017, Simulating the Formation of Ganymede's Grooved Terrain in Three Dimensions: Numerical Approach and Preliminary Results, Lunar and Planetary Science Conference, p. 2461.

Boutonnet, A., Varga, G., Rocchi, A., Martens, W., and Mackenzie, R., 2018, JUICE: Consolidated Report on Mission Analysis (CReMA). ESA Document JUI-ESOC-MOC-RP-001.

Bray, V. J., Schenk, P. M., Jay Melosh, H., Morgan, J. V., and Collins, G. S., 2012, Ganymede crater dimensions – Implications for central peak and central pit formation and development: Icarus, v. 217, no. 1, p. 115-129.

Bruzzone, L., and Croci, R., Radar for Icy Moon Exploration (RIME), *in* Proceedings 2019 IEEE 5th International Workshop on Metrology for AeroSpace (MetroAeroSpace)19-21 June 2019 2019, p. 330-333.

Bruzzone, L., Plaut, J. J., Alberti, G., Blankenship, D. D., Bovolo, F., Campbell, B. A., Ferro, A., Gim, Y., Kofman, W., Komatsu, G., McKinnon, W., Mitri, G., Orosei, R., Patterson, G. W., Plettemeier, D., and Seu, R., 2013, RIME: Radar for Icy Moon Exploration, European Planetary Science Congress, p. EPSC2013-2744.

Cameron, M. E., Smith-Konter, B. R., Collins, G. C., Patthoff, D. A., and Pappalardo, R. T., 2019, Tidal stress modeling of Ganymede: Strike-slip tectonism and Coulomb failure: Icarus, v. 319, p. 99-120.

Cappuccio, P., Hickey, A., Durante, D., Di Benedetto, M., Iess, L., De Marchi, F., Plainaki, C., Milillo, A., and Mura, A., 2020, Ganymede's gravity, tides and rotational state from JUICE's 3GM experiment simulation, v. 187, p. 104902.

Clark, R. N., Curchin, J. M., Hoefen, T. M., and Swayze, G. A., 2009, Reflectance spectroscopy of organic compounds: 1. Alkanes: Journal of Geophysical Research: Planets, v. 114, no. E3.

Collins, G. C., 2006, Global expansion of Ganymede derived from strain measurements in grooved terrain, Lunar Planet. Sci. Conf. XXXVII, Volume abstract no. 2077: Houston, TX: Lunar and Planetary Institute.

Collins, G. C., Head, J. W., and Pappalardo, R. T., 1998, Formation of Ganymede Grooved Terrain by Sequential Extensional Episodes: Implications of Galileo Observations for Regional Stratigraphy: Icarus, v. 135, no. 1, p. 345-359.

Collins, G. C., Patterson, G. W., Head, J. W., Pappalardo, R. T., Prockter, L. M., Lucchitta, B. K., and Kay, J. P., 2013, Global geologic map of Ganymede, p. 3237.

de Kleer, K., Butler, B., de Pater, I., Gurwell, M. A., Moullet, A., Trumbo, S., and Spencer, J., 2021, Ganymede's Surface Properties from Millimeter and Infrared Thermal Emission: The Planetary Science Journal, v. 2, no. 1, p. 5.

Delitsky, M. L., and Lane, A. L., 1998, Ice chemistry on the Galilean satellites: Journal of Geophysical Research: Planets, v. 103, no. E13, p. 31391-31403.

Della Corte, V., Noci, G., Turella, A., Paolinetti, R., Zusi, M., Michaelis, H., Soman, M., Debei, S., Castro, J. M., Herranz, M., Amoroso, M., Castronuovo, M., Holland, A., Lara, L. M., Jaumann, R., and Palumbo, P., Scientific objectives of JANUS Instrument onboard JUICE mission and key technical solutions for its Optical Head, *in* Proceedings 2019 IEEE 5th International Workshop on Metrology for AeroSpace (MetroAeroSpace)19-21 June 2019 2019, p. 324-329.

Della Corte, V., Schmitz, N., Zusi, M., Castro, J. M., Leese, M., Debei, S., Magrin, D., Michalik, H., Palumbo, P., Jaumann, R., Cremonese, G., Hoffmann, H., Holland, A., Lara, L. M., Fiethe, B., Friso, E., Greggio, D., Herranz, M., Koncz, A., Lichopoj, A., Martinez-Navajas, I., Mazzotta Epifani, E., Michaelis, H., Ragazzoni, R., Roatsch, T., Rodrigo, J., Rodriguez, E., Schipani, P., Soman, M., and Zaccariotto, M., The JANUS camera onboard JUICE mission for Jupiter system optical imagingAugust 01, 2014 2014, Volume 9143, p. 91433I.

Di Benedetto, M., Cappuccio, P., Molli, S., Federici, L., and Zavoli, A. J. a. e.-p., 2021, Analysis of 3GM Callisto Gravity Experiment of the JUICE Mission, p. arXiv:2101.03401.

Dirkx, D., Gurvits, L. I., Lainey, V., Lari, G., Milani, A., Cimò, G., Bocanegra-Bahamon, T. M., and Visser, P. N. A. M., 2017, On the contribution of PRIDE-JUICE to Jovian system ephemerides: Planetary and Space Science, v. 147, p. 14-27.

Dombard, A., and McKinnon, W., 2006, Folding of Europa's icy lithosphere: an analysis of viscous-plastic buckling and subsequent topographic relaxation: Journal of Structural Geology, v. 28, no. 12, p. 2259-2269.

Dougherty, M., and al., e., 2014, J-MAG: Magnetometer science on the JUICE mission, EGU General Assembly Conference Abstracts, p. 8791.

ESA JUICE definition study report /Red Book, E. S., 2014, JUICE Jupiter ICy moons Explorer Exploring the emergence of habitable worlds around gas giants, no. ESA/SRE(2014)1.

Fabrizio, D. M., Gaetano, D. A., Giuseppe, M., Paolo, C., Ivan, D. S., Mauro, D. B., and Luciano, I., 2021, Observability of Ganymede's gravity anomalies related to surface features by the 3GM experiment onboard ESA's JUpiter ICy moons Explorer (JUICE) mission, v. 354, p. 114003.

Gladstone, G. R., Retherford, K. D., Egan, A. F., Kaufmann, D. E., Miles, P. F., Parker, J. W., Horvath, D., Rojas, P. M., Versteeg, M. H., Davis, M. W., Greathouse, T. K., Slater, D. C., Mukherjee, J., Steffl, A. J., Feldman, P. D., Hurley, D. M., Pryor, W. R., Hendrix, A. R., Mazarico, E., and Stern, S. A., 2012, Far-ultraviolet reflectance properties of the Moon's permanently shadowed regions, v. 117, p. E00H04.

Gladstone, R., Retherford, K., Eterno, J., Persyn, S., Davis, M., Versteeg, M., Greathouse, T., Persson, K., Dirks, G., Walther, B., Araujo, M., Steffl, A., Schindhelm, E., Spencer, J., McGrath, M., Bagenal, F., Feldman, P., and Fletcher, L., 2013, The Ultraviolet Spectrograph on the JUICE Mission (JUICE-UVS), p. EPSC2013-2394.

Grasset, O., Dougherty, M. K., Coustenis, A., Bunce, E. J., Erd, C., Titov, D., Blanc, M., Coates, A., Drossart, P., Fletcher, L. N., Hussmann, H., Jaumann, R., Krupp, N., Lebreton, J. P., Prieto-Ballesteros, O., Tortora, P., Tosi, F., and Van Hoolst, T., 2013, JUpiter ICy moons Explorer (JUICE): An ESA mission to orbit Ganymede and to characterise the Jupiter system: Planetary and Space Science, v. 78, p. 1-21.

Gurvits, L. I., Bocanegra Bahamon, T. M., Cimò, G., Duev, D. A., Molera Calvés, G., Pogrebenko, S. V., de Pater, I., Vermeersen, L. L. A., Rosenblatt, P., Oberst, J., Charlot, P., Frey, S., and Tudose, V., 2013, Planetary Radio Interferometry and Doppler Experiment (PRIDE) for the JUICE mission, European Planetary Science Congress, p. EPSC2013-2357.

Hansen, G. B., and McCord, T. B., 2004, Amorphous and crystalline ice on the Galilean satellites: A balance between thermal and radiolytic processes: Journal of Geophysical Research, v. 109, no. E1.

Hartogh, P., Barabash, S., Beaudin, G., Börner, P., Bockeleé-Morvan, D., Boogaerts, W., Cavalié, T., Christensen, U. R., Dannenberg, A., Eriksson, P., Fränz, M., Fouchet, T., Frisk, U., Hocke, K., Janssen, C., Jarchow, C., Kasai, Y., Kikuchi, K., Krieg, J.-M., Krupp, N., Kuroda, T., Lellouch, E., Loose, A., Maestrini, A., Manabe, T., Medvedev, A. S., Mendrok, J., Miettinen, E. P., Moreno, R., Murk, A., Murtagh, D., Nishibori, T., Rengel, M., Rezac, L., Sagawa, H., Steinmetz, E., Thomas, B., Urban, J., and Wicht, J., 2013, The Submillimetre Wave Instrument on JUICE, European Planetary Science Congress, p. EPSC2013-2710.

Heggy, E., Scabbia, G., Bruzzone, L., and Pappalardo, R. T., 2017, Radar probing of Jovian icy moons: Understanding subsurface water and structure detectability in the JUICE and Europa missions, v. 285, p. 237.

Hibbitts, C. A., Hansen, G. B., McCord, T. B., and Stephan, K., 2003a, Dark ray crater material on Ganymede - a 1 to 5-μm perspective, EGS - AGU - EUG Joint Assembly.

Hibbitts, C. A., Hansen, G. B., McCord, T. B., Stephan, K., and Stansbery, E., 2003b, Impactor Contamination of Dark Ray Craters on Ganymede, *in* Mackwell, S., ed., Lunar and Planetary Science Conference, Volume 34.

Hibbitts, C. A., Klemaszewski, J. E., McCord, T. B., Hansen, G. B., and Greeley, R., 2002, CO2-rich impact craters on Callisto: J. Geophys. Res., v. 107, no. E10, p. 5084.

Hussmann, H., Lingenauber, K., Kallenbach, R., Enya, K., Thomas, N., Lara, L. M., Althaus, C., Araki, H., Behnke, T., Castro-Marin, J. M., Eisenmenger, H., Gerber, T., Herranz de la Revilla, M., Hüttig, C., Ishibashi, K., Jiménez-Ortega, J., Kimura, J., Kobayashi, M., Lötzke, H.-G., Lichopoj, A., Lüdicke, F., Martínez-Navajas, I., Michaelis, H., Namiki, N., Noda, H., Oberst, J., Oshigami, S., Rodríguez García, J. P., Rodrigo, J., Rösner, K., Stark, A., Steinbrügge, G., Thabaut, P., del Togno, S., Touhara, K., Villamil, S., Wendler, B., Wickhusen, K., and Willner, K., 2019, The Ganymede laser altimeter (GALA): key objectives, instrument design, and performance, v. 11, p. 381.

Hussmann, H., Lingenauber, K., Michaelis, H., Kobayashi, M., Thomas, N., Lara, L., Araki, H., Behnke, T., Gwinner, K., Namiki, N., Noda, H., Oberst, J., Roatsch, T., Rodrigo, R., Sasaki, S., Seiferlin, K., Spohn, T., Althaus, C., Barnouin, O., Beck, T., Breuer, D., Casotto, S., Castro, J. M., Choblet, G., Christensen, U., Ferraz-Mello, S., Giese, B., Kallenbach, R., Kimura, J., Kurita, K., Lainey, V., Lichopoj, A., Lötzke, H.-G., Lüdicke, F., Lupovka, V., Moore, W. B., Rodriguez, A., Santovito, M.-R., Schreiber, U., Schrödter, R., Sohl, F., del Togno, S., Vermeersen, B., Wickhusen, K., Wieczorek, M., and Yseboodt, M., 2013, The Ganymede Laser Altimeter (GALA) as part of the JUICE payload: instrument, science objectives and expected performance, European Planetary Science Congress, p. EPSC2013-2428.

Iess, L., 2013, 3GM: Gravity and Geophysics of Jupiter and the Galilean Moons, European Planetary Science Congress, p. EPSC2013-2491.

Ilyushin, Y. A., and Hartogh, P., 2020, Submillimeter Wave Instrument radiometry of the Jovian icy moons. Numerical simulation of the microwave thermal radiative transfer and Bayesian retrieval of the physical properties, v. 644, p. A24.

Johnson, R. E., 1997, Polar "Caps" on Ganymede and Io Revisited: Icarus, v. 128, no. 2, p. 469-471.

Johnson, R. E., Carlson, R. W., Cooper, J. F., Paranicas, C., Moore, M. H., and Wong, M. C., 2007, Radiation Effects on the Surfaces of the Galilean Satellites, Jupiter, p. 485.

Kay, J. E., and Head, J. W. I., Geologic Mapping of the Ganymede G8 Calderas Region: Evidence for Cryovolcanism, *in* Proceedings LPSC XXX, Houston, TX, March 15-29, 1999 1999.

Khurana, K. K., Pappalardo, R. T., Murphy, N., and Denk, T., 2007, The origin of Ganymede's polar caps: Icarus, v. 191, no. 1, p. 193-202.

Kivelson, M. G., Khurana, K. K., Russell, C. T., Walker, R. J., Warnecke, J., Coroniti, F. V., Polanskey, C., Southwood, D. J., and Schubert, G., 1996, Discovery of Ganymede's magnetic field by the Galileo spacecraft: Nature, v. 384, no. 6609, p. 537-541.

Langevin, Y., and Piccioni, G., 2017, The MAJIS visible/NIR imaging spectrometer on board the ESA JUICE mission : updated design, implications for performances and science goals: European Planetary Science Congress, v. 11.

Langevin, Y., Piccioni, G., Filacchione, G., Poulet, F., and Dumesnil, C., 2018, MAJIS, the VIS-IR imaging spectrometer of JUICE: Information Processing and Management.

Ligier, N., Paranicas, C., Carter, J., Poulet, F., Calvin, W. M., Nordheim, T. A., Snodgrass, C., and Ferellec, L., 2019, Surface composition and properties of Ganymede: Updates from ground-based observations with the near-infrared imaging spectrometer SINFONI/VLT/ESO: Icarus, v. 333, p. 496.

Ligier, N., Poulet, F., Carter, J., Brunetto, R., and Gourgeot, F., 2016, VLT/SINFONI Observations of Europa: New Insights into the Surface Composition: The Astronomical Journal, v. 151, p. 163.

Lucchitta, B. K., 1980, Grooved terrain on Ganymede: Icarus, v. 44, no. 2, p. 481-501.

Luttrell, K., and Sandwell, D., 2006, Strength of the lithosphere of the Galilean satellites: Icarus, v. 183, p. 159-167.

Moore, J. M., Asphaug, E., Morrison, D., Spencer, J. R., Chapman, C. R., Bierhaus, B., Sullivan, R. J., Chuang, F. C., Klemaszewski, J. E., Greeley, R., Bender, K. C., Geissler, P. E., Helfenstein, P., and Pilcher, C. B., 1999, Mass Movement and Landform Degradation on the Icy Galilean Satellites: Results of the Galileo Nominal Mission: Icarus, v. 140, no. 2, p. 294-312.

Moore, J. M., Chapman, C. R., Bierhaus, E. B., Greeley, R., Chuang, F. C., Klemaszewski, J., Clark, R. N., Dalton, J. B., Hibbitts, C. A., Schenk, P. M., Spencer, J. R., and Wagner, R., 2004, Callisto, *in* Bagenal, F., Dowling, T. E., and McKinnon, W. B., eds., Jupiter: The planet, satellites and magnetosphere,: Cambridge, U.K., Cambridge Univ. Press, p. 397 – 426.

Murchie, S. L., and Head III, J. W., 1986, Global reorientation and its effect on tectonic patterns on Ganymede: Geophys. Res. Lett., v. 13, no. 4, p. 345–348.

Palumbo, P., Jaumann, R., Cremonese, G., Hoffmann, H., Debei, S., Della Corte, V., Holland, A., Lara, L. M., Castro, J. M., Herranz, M., Koncz, A., Leese, M., Lichopoj, A., Magrin, D., Martinez-Navajas, I., Mazzotta Epifani, E., Michaelis, H., Ragazzoni, R., Roatsch, T., Rodriguez, E., Schipani, P., Schmitz, N., Zaccariotto, M., Zusi, M., Adriani, A., Aharonson, O., Bell, J., Bourgeois, O., Capria, M. T., Coates, A., Coustenis, A., Di Achille, G., Forlani, G., van Gasselt, S., Groussin, O., Gwinner, K., Haruyama, J., Hauber, E., Hiesinger, H., Langevin, Y., Lopes, R., Marinangeli, L., Markiewicz, W., Marzari, F., Massironi, M., Mehall, G., Mitri, G., Mottola, S., Oberst, J., Patel, M., Pelizzo, M. G., Popa, C., Poulet, F., Preusker, F., Rodrigo, R., Schneider, N., Simon-Miller, A., Stephan, K., Takahashi, Y., Tosi, F., Vincendon, M., and Wagner, R., 2014, JANUS: The Visible Camera Onboard the ESA JUICE Mission to the Jovian System, Lunar and Planetary Science Conference, Volume 45, p. 2094.

Pappalardo, R. T., and Collins, G. C., 2005, Strained craters on Ganymede: J. Struct. Geol., v. 27, no. 5, p. 827-838.

Pappalardo, R. T., Collins, G. C., Head, J. W., III, Helfenstein, P., McCord, T. B., Moore, J. M., Prockter, L. M., Schenk, P. M., Spencer, J. R., Dowling, T. E., and McKinnon, W. B., 2004, Geology of Ganymede, *in* Bagenal, F., ed., Jupiter. The Planet, Satellites and Magnetosphere, p. 363-396.

Paranicas, C., Hibbitts, C. A., Kollmann, P., Ligier, N., Hendrix, A. R., Nordheim, T. A., Roussos, E., Krupp, N., Blaney, D., Cassidy, T. A., and Clark, G., 2018, Magnetospheric considerations for solar system ice state: Icarus, v. 302, p. 560-564.

Patterson, G. W., Collins, G. C., Head, J. W., Pappalardo, R. T., Prockter, L. M., Lucchitta, B. K., and Kay, J. P., 2010, Global geological mapping of Ganymede: Icarus, v. 207, no. 2, p. 845-867.

Piccioni, G., Tommasi, L., Langevin, Y., Filacchione, G., Tosi, F., Grassi, G., Poulet, F., Dumesnil, C., Degalarreta, C. R., Bini, A., Bugetti, G., Guerri, I., and Rossi, M., Scientific goals and technical challenges of the MAJIS imaging spectrometer for the JUICE mission, *in* Proceedings 2019 IEEE 5th International Workshop on Metrology for AeroSpace (MetroAeroSpace)19-21 June 2019 2019, p. 318-323.

Prockter, L. M., Figueredo, P. H., Pappalardo, R. T., Head, J. W. I., and Collins, G. C., 2000, Geology and mapping of dark terrain on Ganymede and implications for grooved terrain formation

J. Geophys. Res., v. 105, no. E12, p. 29315-29325.

Prockter, L. M., Head, J. W., Pappalardo, R. T., Senske, D. A., Neukum, G., Wagner, R., Wolf, U., Oberst, J., Giese, B., Moore, J. M., Chapman, C. R., Helfenstein, P., Greeley, R., Breneman, H., and Belton, M. J. S., 1998, Dark Terrain on Ganymede: Geological Mapping and Interpretation of Galileo Regio at High Resolution: Icarus, v. 135, no. 1, p. 317-344.

Rossi, C., Cianfarra, P., Salvini, F., Mitri, G., and Massé, M., 2018, Evidence of transpressional tectonics on the Uruk Sulcus region, Ganymede: Tectonophysics, v. 749, p. 72-87.

Sbalchiero, E., Thakur, S., and Bruzzone, L., 3D radar sounder simulations of geological targets on Ganymede Jovian MoonOctober 01, 2019 2019, Volume 11155, p. 111551J.

Schenk, P. M., 1995, The Geology of Callisto: Journal of Geophysical Research, v. 100, p. 19023-19040.

-, 2002, Thickness constraints on the icy shells of the galilean satellites from a comparison of crater shapes: Nature, v. 417, p. 419-421.

Schenk, P. M., Asphaug, E., McKinnon, W. B., Melosh, H. J., and Weissman, P. R., 1996, Cometary Nuclei and Tidal Disruption: The Geologic Record of Crater Chains on Callisto and Ganymede: Icarus, v. 121, no. 2, p. 249-274.

Schenk, P. M., Chapman, C. R., Zahnle, K., and Moore, J. M., 2004, Ages and interiors: the cratering record of the Galilean satellites, *in* Bagenal, F., Dowling, T. E., and McKinnon, W. B., eds., Jupiter: The planet, satellites and magnetosphere: Cambridge, UK, Cambridge University Press, p. 427 - 456.

Schenk, P. M., and McKinnon, W. B., 1991, Dark-ray and dark-floor craters on Ganymede, and the provenance of large impactors in the Jovian system: Icarus, v. 89, p. 318-346.

Schenk, P. M., McKinnon, W. B., Gwynn, D., and Moore, J. M., 2001, Flooding of Ganymede's bright terrains by low-viscosity water-ice lavas: Nature, v. 410, p. 57-60.

Schenk, P. M., and Moore, J. M., 1995, Volcanic constructs on Ganymede and Enceladus: Topographic evidence from stereo images and photoclinometry: Journal of Geophysical Research, v. 100, p. 19009-19022.

Smith, B. A., Soderblom, L. A., Beebe, R., Boyce, J., Briggs, G., Carr, M., Collins, S. A., Cook, A. F., Danielson, G. E., Davies, M. E., Hunt, G. E., Ingersoll, A., Johnson, T. V., Masursky, H., McCauley, J., Morrison, D., Owen, T., Sagan, C., Shoemaker, E. M.,

Strom, R., Suomi, V. E., and Veverka, J., 1979, The Galilean Satellites and Jupiter: Voyager 2 Imaging Science Results: Science, v. 206, no. 4421, p. 927-950.
Spaun, N. A., Head, J. W., III, Pappalardo, R. T., and Team, G. S., 2001, Scalloped Depressions on Ganymede from Galileo (G28) Very High Resolution Imaging, Lunar and Planetary Science Conference, Volume 32.
Spencer, J. R., 1987, Icy Galilean satellite reflectance spectra: Less ice on Ganymede and Callisto?: Icarus, v. 70, no. 1, p. 99-110.
Squyres, S. W., 1980, Surface temperatures and retention of H2O frost on Ganymede and Callisto: Icarus, v. 44, p. 502-510.
Stephan, K., Hibbitts, C. A., and Jaumann, R., 2020, H2O-ice particle size variations across Ganymede's and Callisto's surface: Icarus, v. 337, p. 113440.
Thakur, S., and Bruzzone, L., 2020, Subsurface radar evidence of cryovolcanic resurfacing on the Jovian moon Ganymede: RIME detectability analysis, p. EPSC2020-2259.
Thakur, S., and Bruzzone, L., 2021, An Approach to the Generation and Analysis of Databases of Simulated Radar Sounder Data for Performance Prediction and Target Interpretation: IEEE Transactions on Geoscience and Remote Sensing, p. 1-19.
Trumbo, S. K., Brown, M. E., and Hand, K. P., 2019, Sodium chloride on the surface of Europa: Science Advances, v. 5, no. 6, p. eaaw7123.
Van Der Plas, P., and Nespoli, F., 2016, MAPPS: a Science Planning tool supporting the ESA Solar System Missions, SpaceOps 2016 Conference: Daejon, Korea.
Vorburger, A., Pfleger, M., Lindkvist, J., Holmström, M., Lammer, H., Lichtenegger, H. I. M., Galli, A., Rubin, M., and Wurz, P., 2019, Three-Dimensional Modeling of Callisto's Surface Sputtered Exosphere Environment, v. 124, no. 8, p. 7157-7169.
Wagner, R. J., Schmedemann, N., Werner, S. C., Head, J. W., Stephan, K., Krohn, K., Jaumann, R., Roatsch, T., Hoffmann, H., and Palumbo, P., 2019a, Ray Craters on Ganymede as Time-Stratigraphic Markers, Lunar and Planetary Science Conference, p. 1849.
Wagner, R. J., Schmedemann, N., Werner, S. C., Head, J. W., Stephan, K., Krohn, K., Roatsch, T., Hoffmann, H., Jaumann, R., and Palumbo, P., 2019b, Ray Craters as Stratigraphic Markers in Ganymede's Geologic History, EGU General Assembly Conference Abstracts, p. 7208.
Wirström, E. S., Bjerkeli, P., Rezac, L., Brinch, C., and Hartogh, P., 2020, Effect of the 3D distribution on water observations made with the SWI. I. Ganymede, v. 637, p. A90.
Wurz, P., Meyer, S., Galli, A., Tulej, M., Vorburger, A., Lasi, D., Piazza, D., Lüthi, M., Brandt, P., and Barabash, S., 2018, The Neutral Gas and Ion Mass Spectrometer of the PEP Experiment on the JUICE Mission, EGU General Assembly Conference Abstracts, p. 10091.
Zahnle, K., Schenk, P., Levison, H., and Dones, L., 2003, Cratering rates in the outer solar system: Icarus, v. 163, p. 263–289.